ANALYSIS OF NDVI- TIME SERIES TO DETECT BUSH ENCROACHMENT: A case study in Cadiz (Spain) assessing three different methods on the basis of minimum NDVI

Lina M. Estupiñan-Suarez

May, 2013

Course Title:	Geo-Information Science and Earth Observation for Environmental Modeling and Management
Level:	Master of Science (MSc)
Course Duration:	August 2011 – June 2013
Consortium Partners:	Lund University (Sweden) University of Twente, Faculty ITC (The Netherlands) University of Southampton (UK) University of Warsaw (Poland) University of Iceland (Iceland) University of Sydney (Australia, Associate Partner)

ANALYSIS OF NDVI- TIME SERIES TO DETECT BUSH ENCROACHMENT: A case study in Cadiz (Spain) assessing three different methods on the basis of minimum NDVI

by

Lina M. Estupiñan-Suarez

Thesis submitted to the Faculty of Geoinformation Science and Earth Observation, University of Twente, in partial fulfilment of the requirements for the degree of Master of Science in Geo-information Science and Earth Observation for Environmental Modelling and Management

Thesis Assessment Board

Chair: Dr. Y. H. Hussin
External Examiner: Dr. R.H.G. Jongman (Alterra – Wageningen University)
1st Supervisor: Dr. A.G. Toxopeus
2nd Supervisor: Dr. ir. C.A.J.M. de Bie

UNIVERSITY OF TWENTE.
ITC
FACULTY OF GEO-INFORMATION SCIENCE AND EARTH OBSERVATION

Disclaimer

Abstract

Encroachment is an ecological succession process where perennial plants such as bushes and trees replace annual vegetation. In general, bushes establishment increases and the canopy tends to close. This process leads to gradual changes in land cover. Until now, bush encroachment detection using remote sensing has required high spatial resolution. This study aimed to investigate three different methods which use moderate spatial resolution time series of MODIS-NDVI 250m from 2001 to 2012. It pursued to differentiate between bushes (evergreen perennial cover) and annual vegetation cover. For that purpose, the assessed dataset was constrained to the three NDVI composites that hold the lowest NDVI values (min.NDVI) for each year. The three evaluated methods were: (a) CoverCAM, (b) Cover Fraction and (c) Quantile Linear Regression (QuantReg). All of them were based on min.NDVI time series. The study area was the province of Cadiz (Spain) where land degradation and land abandonment has increased, two of the major causes of encroachment. The findings revealed that the potential use of minimum NDVI to detect bush encroachment varies among methods. The method with highest accuracy is QuantReg (PCC=0.77) and its bush encroachment detection is 0.82 (Sensitivity). CoverCAM and Cover-Fraction showed a low power of detection. It is concluded that QuantReg is a robust approach for bush encroachment detection and has potential application in surveying large areas.

Acknowledgements

This work is the capstone of two years full of nice and sometimes hard experiences. First at all, I thank the GEM MSc course and Erasmus Mundus fellowship for give me the opportunity to join this master program. The education in Lund University found my GIS basis for a better professional development in ITC.

My deepest appreciation goes to my both supervisors. Bert, I thank you for all the support and motivation during the thesis process. Your always ecological perspective provided me a new overview of the study. Kees, I will always remember your teachings about consistency and logic in a research. Furthermore, your guide in the methodology was essential for the construction of this work. In addition, I want to thank Karin Larson, my first GIS professor, from Lund University, who not only is an excellent professor but also is opened to advice all the students.

I also express my gratitude to people who contribute in one way or another to my thesis. In the beginning, I counted with the help of Amjad Ali and Willem Nieuwenhuis who kindly contributed to the development of my methods. In the same way, to Nuno César Du Sá who was my second hand during the fieldwork; you always supported me and gave me motivation. As well, professors Raimundo Real, Antonio Roman, University of Malaga, Junta de Andalusia and Fundacion Migres who helped us in our stay in Spain. Mafe, Effie, Islam and Nina, you all became fundamental in the end of this study. Thank you for your time discussing with me, giving me advices and comments. All of them were very appreciated.

It is impossible not to mention my home university Universidad Nacional de Colombia and professors Orlando Vargas and Edgar Cristancho who were essential in my way to my postgraduate. They have not only been my academic mentors but also they have become my advisors. Each of you has contributed widely to my scientific background and my positive self-development.

And now, I am afraid that the words are not going to be enough... My dear GEM family, your four have just become part of myself. You were with me during this two years, in Lund and in Enschede, and sooner or later you touched my heart and you can be sure that you will remain there forever: Joana, your charming made my days happier, Shrota; your kindness is just contagious, Joaquín, I sincerely feel your support and unconditional friendship. Collins, your words were always appropriate and touching for everybody. To be with you guys was one of the best things I had in Europe!

Xime, Liz, Luisa and Dani; you know the best and the worst part of myself. Thank you for being next to me even with thousands miles of distance, for all the support and your friendship through all these years, for listening to me and share the sweet and the sour of my live.

Finally, all my love and gratitude to my mom (*mami* Nidya Suarez), Mile and Pablis, you three share my dreams, hold my hand and stand by my in all decisions I make. As well to Is, Flor, Cony and all my Estupiñan-Rojas and Suarez-Camacho family that have been looking after me all this time.

This work is warmly dedicated
To a women of courage and wisdom, Nidya Suárez, my mom
To a smart, truthful and well-remembered man, Antonio Estupiñán, my dad
To my loved lawyer and computer engineer, my siblings,
Milena and Juan Pablo Estupiñán-Suárez
To the welcome youngest Julieta Nanu

Table of Contents

List of Figures

List of Tables

List of Acronyms

CoverCAM = Cover Composition Assessment Method

DN = Digital Numbers, from 0-255, it is the new scale of NDVI values after it has been rescaled.

min.NDVI= minimum NDVI. 3 year composites from July 28th to September 13th. 36 composites in total from 2001 to 2012

MODIS= Moderate resolution Imaging Spectroradiomeer

NDVI= Normalized Difference Vegetation Index

PCC=Percentage Correct Classified pixels

Se=Sensitivity

SD= Standard deviation

SDp= Pooled standard deviation

Sp=Specificity

VI= Vegetation Indices

Glossary

Annual vegetation= In this study, annual vegetation has been defines as plants that die, dry out or are absent during summer therefore they do not photosynthesize i.e. grass, herbs, phenomena observed in Mediterranean ecosystems

Change pixels= Surveyed pixels during calibration or validation with an increase of perennial cover or in other words bush encroachment

Composite, MODIS = It is a satellite image compose of daily NDVI images of 16 days. Satellite product provided by NASA.

Land Cover Classes: Three land cover classes were defined: grasslands-rangelands, scrublands and forest. Residential and agricultural lands were masked out.

Min.NDVI= Subset of three NDVI composites, values from August 28th to September 13th.

No-Change pixels= Surveyed pixels during calibration or validation with no increase of perennial cover.

Perennial vegetation= In this study, perennial vegetation exclusively refers to evergreen perennial plants that do photosynthesize the whole year. The evergreen perennial vegetation is typical of Mediterranean ecosystem and deciduous vegetation is not observed frequently.

Summer NDVI= Subset of NDVI composites images; from May 25th to October 15th.

Vegetation Cover Classes= This study was focused on two vegetation cover classes: perennial vegetation and annual vegetation

Chapter 1. Introduction

1.1 Motivation of the Study

Encroachment is a natural regeneration process that occurs in open areas produced after fire, flooding, etc., or when lands have been abandoned. During encroachment woody plants establishment increases and the canopy tends to close. This ecological process occurs gradually and must be consistent across time to generate changes in the ecosystem (Verburg et al. 2006, Sluiter and de Jong 2007). Its identification through remote sensing is challenging because it is linked to high variability in the data and occurs locally at small spatial and temporal scale. Additionally, each evaluated pixel is under different conditions and is considered as a different study case. Therefore, each pixel has a specific vegetation composition and cover density. Until now, high spatial resolution has been used to surveyed areas with encroachment (McGlynn and Okin 2006, Oldeland et al. 2010). This study aimed to investigate three different methods which use moderate spatial resolution. Two cover composition classes; (i) evergreen perennial vegetation bushes and trees and (ii) annual vegetation which is herbs or grass. Areas covered by annual plants plus patches of bushes and trees are vulnerable to encroachment if conditions are favorable.

Vegetation monitoring, using remote sensing, has been mainly based on analysis of vegetation indices (VI) and is implemented to survey large areas with abrupt changes i.e. deforestation, natural disasters, agriculture yield and calendars (Lunetta et al. 2006, De Bie et al. 2008). Nevertheless detection of gradual changes in vegetation composition like encroachment is limited. VI are able to bring information about vegetation state but less about vegetation density cover. Also, they are susceptible to floristic composition (plant diversity). One of the main differences of VI among pixels with similar vegetation cover density is explained by vegetation composition. For example, sclerophyllus vegetation, pinus and broadleaf trees are all evergreen plants with clear differences in their leaves structure and physiology, which leads to significant variation in their VI (Soudani et al. 2012, Hmimina et al. 2013).

It is clear that encroachment is a particular process that leads gradual change in land cover (McGlynn and Okin 2006, Oldeland et al. 2010). This research aimed to develop a method to detect pixels with bush encroachment looking at consistent patterns of VI through time. The study is challenging because it is a pixel level analysis and the imagery has moderate resolution (MODIS-NDVI 250m 16-days composite) besides interannual variation of VI.

For that reason, a method in development (Method A) and two new approaches were proposed (Method B and C) to find distinct data trends between pixels with bush encroachment (Change pixels) and constant pixels

(No-Change pixels). Furthermore, time periods that enhance the difference of perennial and annual cover were sought.

Three methods were selected to either perform a comparison between reference and monitoring period (Method A) or to compare between Change and No-Change pixels (Methods B and C).

To reach this objective, the research approach was based on:

- Time series analysis of VI because it reveals information of vegetation dynamics and on-going processes e.g. phenology.
- The evaluation of two vegetation cover composition classes: (1) Annual Vegetation which includes herbs and grass; and (2) Evergreen Perennial Vegetation which is plants such as shrubs and trees.
- The lowest values of VI because they enhance the difference between perennial and annual vegetation for the case study (Cadiz, Spain). These values are obtained in summer when evergreen perennial vegetation remains with leaves and is the only vegetation doing photosynthesis. Otherwise, annual vegetation loses leaves, dry out or is dead in summer, hence it has null photosynthesis activity.
- A dataset constrained to three Normalized Difference Vegetation Index (**NDVI**) composites called from now on **min.NDVI**; these composites hold exclusively NDVI from perennial vegetation because annual vegetation is absent. The evaluated period is from July 28th to September 13th.

In this study, detection of bush encroachment was focused on the increase of evergreen perennial cover at pixel level. It was expected that evergreen perennial vegetation replace annual vegetation in areas vulnerable to encroachment. For this research, perennial vegetation exclusively refers to evergreen perennial vegetation. In general, the bushes and trees in the Mediterranean ecosystem are adapted to dry conditions and have leaves all the year round, examples of this is the Maquis and sclerophyllous vegetation (Terradas 1991). The assumption made was that areas covered with grass and herbs will experience a min.NDVI increment during summer when they are being colonized by bushes. Then, three methods were proposed to explore the min.NDVI time profiles from 2001 to 2012. Furthermore, bush encroachment detection accuracy and performance were assessed. To diminish recognition of abrupt change, agricultural and urban areas were excluded from this study because they have high anthropogenic influence and are not favorable for encroachment.

1.2 Literature Review

Ecosystems are dynamic in space and time. They are exposed to intra-annual and interannual climatic regimes and variations. Verbesselt et al. (2010) resume ecosystem changes into three classes: seasonal, abrupt and gradual change. Seasonality determines phenological and physiological changes. For example, photosynthesis rate increases in the rainy season and decreases in the dry season. This variation is intrinsic to the system dynamic and does not cause any significant change. However, abrupt and gradual changes lead to exceed the system's resilience generating new vegetation composition and land cover.

Some abrupt changes are urban development and natural hazards. Populated regions are often transformed by humans; infrastructure is expanded (e.g. dams, roads, solar panels) and agricultural practices are technified (Butchart et al. 2010, Pereira et al. 2010, Ellis 2011). In the same way, natural disasters cause land conversion. Wildfire and floods destroy the vegetation cover and generate conditions for plant succession (Scheffer 2001, Zhan et al. 2002, Folke et al. 2004). Depending on disturbance intensity, ecosystems can be recovered to previous states when conditions are favorable. Otherwise, a different ecosystem is established (Connell and Slatyer 1977, Pickett et al. 1987). Alternatively, plant colonization also generates new land cover. Establishment of shrubs and trees is observed on abandoned lands or poor maintained rangelands (Verburg et al. 2006, Sluiter and de Jong 2007). This process is called woody encroachment and occurs gradually (Archer et al. 1995, Lasanta et al. 2001). Its detection is challenging, requires high resolution in time and/or space, whereas abrupt disturbances have a high probability to be detected by remote sensing techniques.

In Europe, environmental policy development and implementation require land cover, land use and land monitoring information. Reduced time delay, quality data and quantitative results are the main concern for European governments. These issues have been partially solved through the application of Geographical Information System (GIS) (Cohen and Goward 2004, Sluiter 2005, Vogiatzakis et al. 2006, Büttner et al. 2012) Satellite images, aerial photography, models, among others, have been used in as a cost effective way to survey large areas (Kerr and Ostrovsky 2003, De Aranzabal et al. 2008). On-going studies have improved methods and products to monitor or detect conversion at landscape scale (Kawabata et al. 2001, Plieninger 2006, Geerken

2009, Stellmes et al. 2010). For example, the combination of baseline maps and SPOT images (1km) produced an improved land use map. The improved map includes crops intensity and performance being appropriate for land monitoring (de Bie et al. 2011). Another application is the detection of deforested areas as a consequence of urbanization and forest harvesting. In this field, Lunetta et al. (2006) developed an automated data processing algorithm which works with MODIS NDVI 250 from 2001 to 2005.

Also, studies of biodiversity, landscape degradation and fragmentation are required (Fischer and Lindenmayer 2007). Species are experiencing reduction of areas for feeding and shelter. Modifications of edaphic properties, water level and climatic regimes disrupt the ecosystems' resilience altering the fauna and flora composition and structure (McIntyre and Hobbs 1999, Fischer and Lindenmayer 2007, Decout et al. 2012). Innovative projects have studied alternatives to increase and maintain areas for wildlife highlighting the importance of abandoned lands. A new initiative is the introduction of wild ungulates in rangelands, occupied previously by cattle, to control woody plants establishment and reduce encroachment (Rewilding Europe 2011). This is an attractive strategy for managing abandoned lands in the Mediterranean basin which is one of the biodiversity hotspots in the world (Marañón et al. 1999, Myers et al. 2000). Its high number of species is mainly found in the agrosilvopastoral systems called *dehesas.* These ecosystems combine trees, scrubs and grasslands generating a mosaic of vegetation which provides microclimates for different species. It is a human made ecosystem, its equilibrium is associated to livestock raising and cork production, important economic activities in Spain and Portugal (Plieninger and Wilbrand 2001, Díaz et al. 2003, Consejeria de Medio Ambiente 2010).

The study area is located in Cadiz Province (Spain). Its natural vegetation cover is a mixture of grassland, scrublands and forest. The perennial vegetation is evergreen while the annual vegetation is dead or is hay in summer (Sanchez-Garcia et al. 2004, Consejeria de Medio Ambiente 2010). Taking into consideration this difference, it was proposed to analyze the min.NDVI because it will enhance NDVI increase caused by perennial cover increase. During min.NDVI composite time, the greenness is exclusive of perennial cover while annual vegetation is absent. This survey is based on time series analysis of NDVI MODIS Terra 250m (version 5 MOD13Q1) which has been appropriate for climate models and land cover surveys at large scales around the world (U. S. Geological Survey 2011).

1.1.1 Land Cover Change Detection and Encroachment

Field surveys in land cover assessments at large scale demand extensive funds and sampling effort; besides they generate time delays (Smith et al. 2011, Hmimina et al. 2013). Land cover classification and change detection has been successfully performed through remote sensing techniques. They have the power of streamline and automated processes for further applications. Vegetation Indices (VI) are the capstone input in this field. For that purpose, the implementation of VI in algorithms development and new approaches have increased. For example, Geerken et al. (2005) used Fourier filters to clean data and regression coefficients to classify rangelands cover type. Verbesselt et al. (2010) proposed a method to decompose NDVI into trend, seasonal and remainder components to detect change in time series, while Hermance et al. (2007) implemented a polynomial spline algorithm to track phenology at short and long term.

The detection of encroachment, using remote sensing, has been limited by imagery resolution and availability. Some studies have compared and combined hyper-temporal with high spatial resolution imagery. Busetto et al. (2008) used high frequency images (NOAA AVHRR) and high spatial resolution (Landsat TM/ETM+) to detect changes in rangelands management. Both imagery demonstrated to be complementary; time series enhance time frequency details and high spatial scale marks fine areas (Busetto et al. 2008, Stellmes et al. 2010).

1.1.2 VI and NDVI: definition, equation and applications

VI are satellite derived products that bring out information of plants biomass and photosynthesis rates. VI are used to measure green vegetation growth up and senesce often known as “greenness”. Frequently, its estimation is affected by atmospheric particles (e.g. water, dust, clouds), ground objects (e.g. soil, litter) and canopy light properties (Huete et al. 1994). Despite these factors, VI have been successfully applied to monitor ecosystems health, land cover, crops production, deforestation and have been implemented in regional and global models (Hickler et al. 2005, Lassau et al. 2005, Lunetta et al. 2006, Smith et al. 2011).

The Normalized Difference Vegetation Index (NDVI) is the most known and used VI. It is the normalized difference between near infrared (NIR) and red reflectance with values from -1 to 1 (Equation 1). Positive values are indicators of green vegetation cover whereas water, clouds or snow have negative values (Taiz and Zeiger 2010, Weier and Herrin 2011). NDVI varies among species and vegetation types. Yellow leaves present low NDVI, pinus and sclerophilus have intermediate to low NDVI values (Soudani et al. 2012, Hmimina et al. 2013).

***Equation* 1**

$$NDVI = \frac{NIR - RED}{NIR + RED}$$

Where NIR is Near Infrared and RED is Red Reflectance

The NDVI principle is based on the absorption of visible light (0.4-0.7µm) by green leaves during the photosynthesis. Chlorophyll is excited by visible light wavelengths, thus a flux of electrons is transmitted through the chloroplast to produce and store energy in the cell. The most absorbed visible light has wavelengths between 0.62 and 0.69 µm which are within the red spectrum. Other parts of the light spectrum as NIR (0.7-1.1µm) are highly reflected by plants (Taiz and Zeiger 2010, Weier and Herrin 2011).

NDVI annual profiles are analyzed to study plant phenology. They bring out information about vegetation health and type. Figure 1a depicts the NDVI profile in 2001 for different classes in Cadiz (Spain). In general, all classes present the same trend, but not the irrigated rice fields (class 6) which are maintained by humans. Forest classes have the highest NDVI and the values do not drop significantly in summer (composites 12 to 19). Rangelands have high NDVI in the rainy season and very low NDVI in the dry season. Depending on the crops, the NDVI patterns vary and even do not follow the normal plants seasonality trend like the rice fields. It is observed that the photosynthesis activity peak occurs between March 22th and May 8th (spring) and then decreases during summer.

Long term studies of NDVI mark vegetation dynamic cover changes or strong variations in climate. Figure 1b shows NDVI time series from 2001 to 2006. The counted number of NDVI peaks or valleys reflects the evaluated number of years, six herein. A marked NDVI decrease is observed in 2005 for all the classes (composites 106-111). This year, Spain experienced a strong drought (AEMET 2012).

NDVI products have been available since 1972, the first satellite in charge was Landsat MSS (79 m) and carried out until 1992. Currently, AVHRR-NOAA (1 km, 8 km), Landsat ETM+ (30 m) SPOT Vegetation (1.15 km) and MODIS Terra/Aqua (250 m, 500 m, 1km) are operating and provide VI data for low or no cost(U. S. Geological Survey 2012). MODIS/Terra 5 version (MOD13Q1) was selected for this study. This satellite has free global coverage imagery and has been corrected for atmospheric and other artifacts e.g. water, clouds distortions. Its accuracy has been successfully assessed with ground control points. The red band has been centered at 645nm and NIR at 858nm. (U. S. Geological Survey 2011).

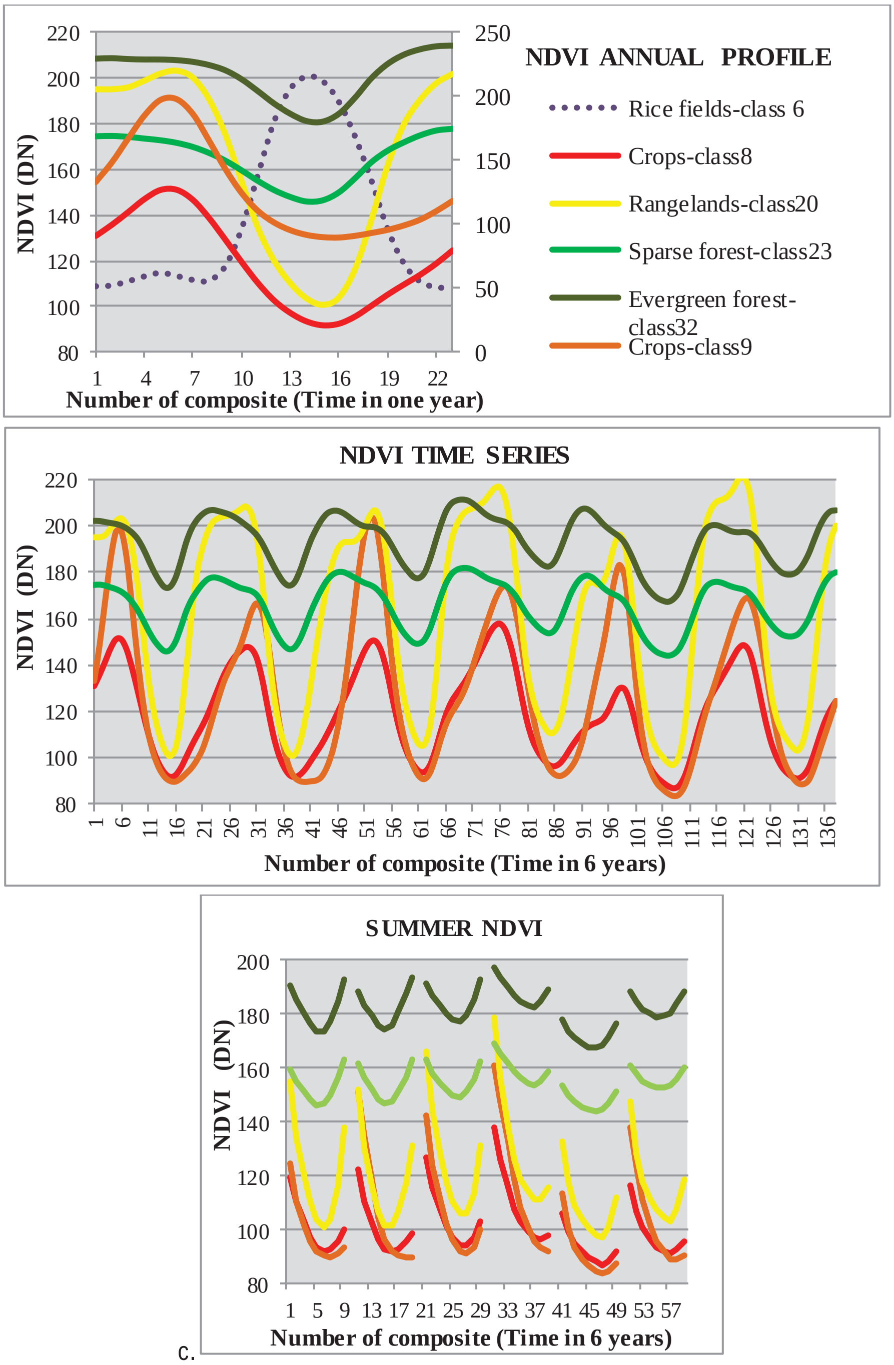

a.

b.

c.

Figure 1. NDVI profiles of different ISODATA classes. a. Annual NDVI profiles 2001. The whole year has 23 NDVI composites and one composite is 16 days. b .NDVI time series from 2001 to 2006. c. Summer NDVI from May 31st to October 15th in 6 years (2001-2006)

1.3 Overview of the min.NDVI concept and its application

Observations in the fieldwork in Cadiz (Spain) pointed out the enhanced difference between perennial and annual cover in summer, and the potential application of VI to assess encroachment looking at NDVI summer values. Figure 1c displays the summer NDVI values from May 31st to October 15th (9 composites). The lowest NDVI values are 3 composites between July 28th and September 13th. Each composite is an aggregation of 16-days NDVI. The first composite is from July 28th to August 12th. The second composite is from August 13th to August 28th and the third one from August 29th to September 13th. This period includes the warmest and driest days in Andalusia where photosynthesis is only performed by perennial vegetation (evergreen leaves).

In this study, the three composites from July 28th to September 13th, mentioned previously were defined as **min.NDVI**. This fraction of NDVI data has been selected for bush detection through 12 years (2001-2012). The min.NDVI dataset was implemented in three different approaches. All assessed methods pursued to flag pixels with high probability of gradual change looking at anomalies of min.NDVI. All methods are:

- Based on the analysis of the same min.NDVI composites stack. An overall of 36 images, 12 years and 3 composites *per* year.
- The change detection is performed at pixel level
- Aerial images from Google™ earth are used to detect changes of perennial cover, to select pixels with and with No-Change and to calibrate the methods.
- The methods accuracy assessment uses the same dataset (n=52). The evaluation imagery is sourced by *La Junta de Andalucia*.

The main differences among methods are:

- CoverCAM (Method A) splits the study time period in two; a reference and monitoring period to include interannual variability. Therefore, the change detection period is only from 2007 to 2012.
- Cover Fraction (Method B) relates NDVI values with perennial cover density and does not consider interannual variability.
- QuantReg (Method C) focuses on the lowest NDVI values from the whole study period reducing climatic effects e.g. very wet or dry years.

- Change detection criteria are selected depending on the method properties.

CoverCAM is based in a complex logic procedure (see methods), whereas Cover Fraction and QuantReg are founded on linear regressions analysis. However, the last two have an important difference. On one hand, Cover Fraction evaluates the linear relation between NDVI and perennial cover and thus it has to fill the assumptions for a parametric test. On the other hand, QuantReg assesses NDVI through time and is a semiparametric statistical technique.

It is relevant to state that this study seeks to validate the significance of min.NDVI to detect gradual change cover. The priority is to find out if this fraction of the NDVI annual profile is meaningful and has a potential use to recognize areas with encroachment. Secondly, it is aimed to compare the methods performance to propose their future application but it does not intend to evaluate or quantify how different the methods are from each other.

Hence, the power of the methods to detect bush encroachment was based on accuracy measurements of the confusion matrix. (1) The percentage of corrected classified pixels **(PCC)** which is the number of corrected pixels predictions divided by the total number of pixels. PCC brings out information of the overall number of correctly predictions and is highly affected but high values of Sensitivity (**Se**) or Specificity (**Sp**). The method **Se** (2) is the number of correctly predictions of Change pixels overall predicted Change pixels, it means correctly and incorrectly predictions. The method **Sp** (3) is the number of correctly predicted No-Change pixels overall predicted pixels as No-Change pixels, it means correctly and incorrectly predictions. (Lillesand et al. 2008). The assessment of all of them, lead to a correct interpretation of the method performances.

Chapter 2. Research Approach

2.1 Research Questions

- Can minimum NDVI be used to detect bush encroachment?
- Does minimum NDVI significantly differ between pixels with bush encroachment (change) and without (No-Change pixels)?

2.2 Research Objective

2.2.1 General Objective

- To assess the performance of three methods to detect bush encroachment based on minimum NDVI data and their overall accuracy.

2.2.2 Specific Objectives

- To assess bush encroachment detection by CoverCAM (method A) using minimum NDVI data.
- To assess bush encroachment detection by Cover-Fraction (method B) using minimum NDVI data and perennial cover.
- To assess bush encroachment detection of QuantReg (method C) based on minimum NDVI.
- To discuss the difference among methods and their performance

2.3 Hypothesis

Hypothesis 1

The Method[i] has a significant prediction of Change and No Change pixels in natural areas of Cadiz (Spain)

Ho: PCC Method$_{[i]}$ $\leq$ 0.75
Ha: PCC Method$_{[i]}$ > 0.75
Where i is method A or B or C,
PCC is predicted corrected classified
And 0.75 is the threshold decision made by the research

Hypothesis 2

The Method[i] significantly predicts bush encroachment (change pixels) in natural areas of Cadiz (Spain)

Ho: Method$_{[i]}$ *Se* $\leq$ 0.75
Ha: Method$_{[i]}$ *Se* > 0.75
Where i is method A or B or C and
Se is Sensitivity
and 0.75 is the threshold decision made by the research

Chapter 3. Methodology

3.1 Methodology overview

This study was divided in three main phases. The first phase included literature review and the exploration of the study area. Data acquisition, pre-processing and the preparation of the study area mask were also performed in this phase. The second phase was the construction of the calibration and validation datasets through image visualization, estimation of perennial cover and the exportation of min.NDVI profiles. The last phase was calibration of the three methods, validation and their final comparison. Figure 2 and Figure 3 show in detail each phase but explanations of all steps are explained in the next sections.

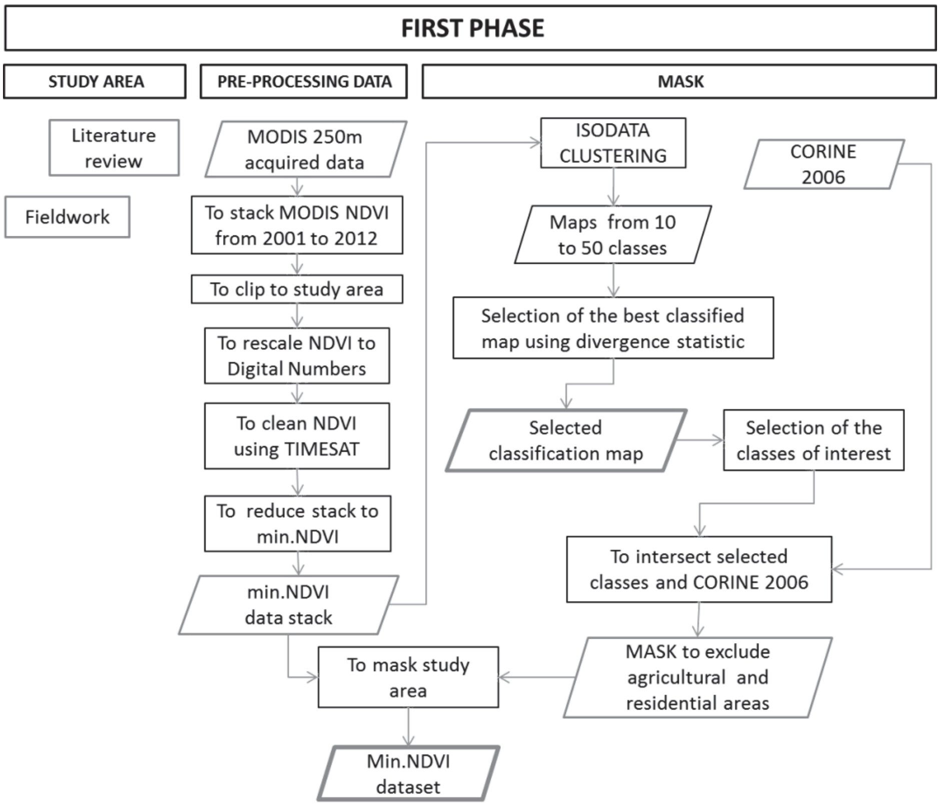

Figure 2. Flowchart methodology Phase 1.

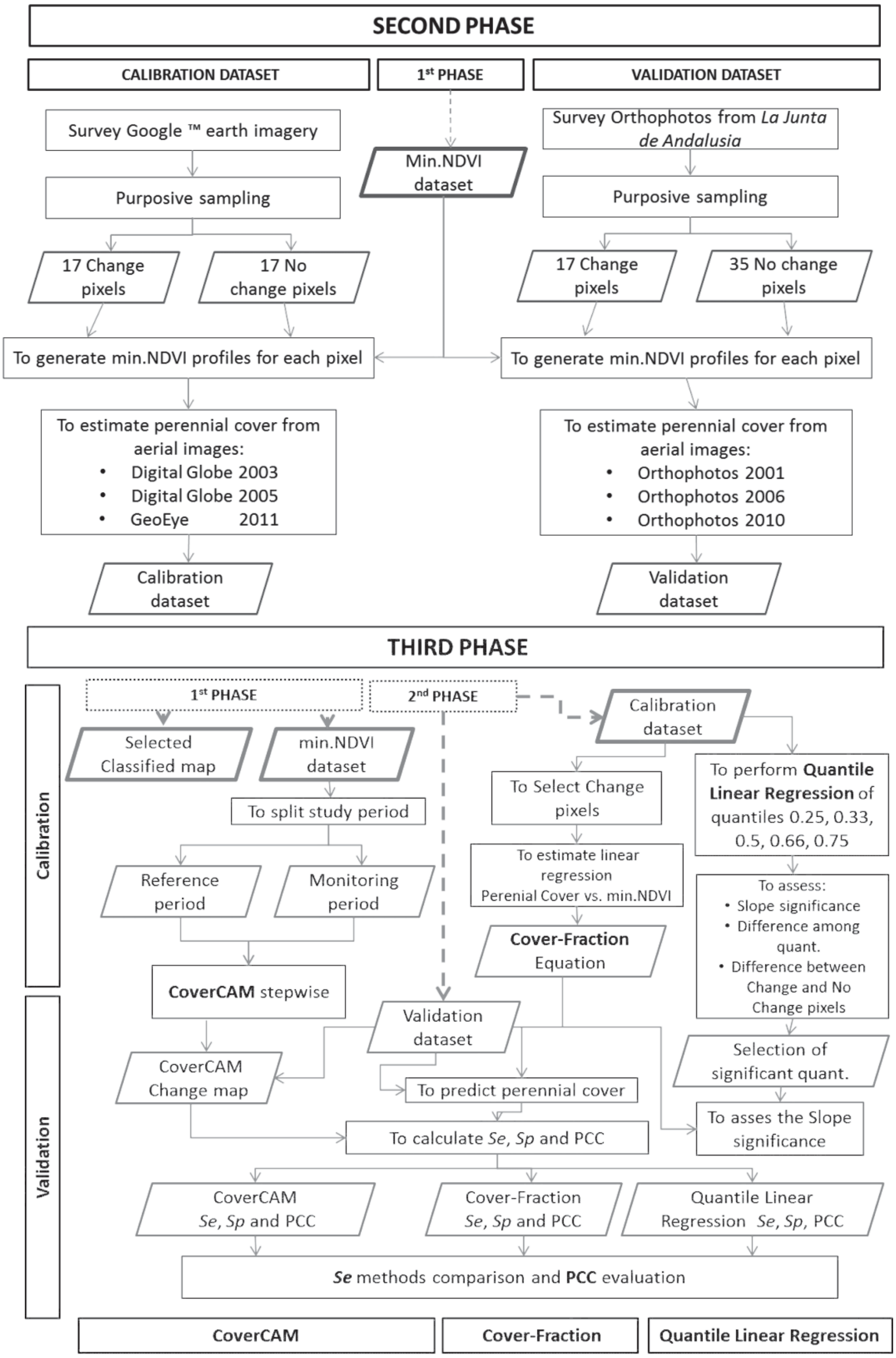

Figure 3. Flowchart Methodology. Top: Phase 2 Bottom: Phase 3. Dotted lines introduce outputs from previous phases Se=Sensitivity Sp=Specificity PCC=PredictionCorrected Classified

3.2 Study Area

The study area includes almost all the Cadiz Province and a small part of the South West of Malaga Province. Both provinces belong to Andalusia region located in the Southern part of Spain. Cadiz has an area of 744.200 hectares. Its main land covers are forestall areas (185.138 ha), croplands (185.138 ha), and grasslands (141.876 ha) (Consejería de Agricultura y Pesca 2003). The main productive activities in order of importance are tourism (70%); industry, energy, construction (26.2%); and agriculture, cattle farming and fishing (3.8%). The current population in the province is 1.236.739 with just an increment of 230.636 habitants in the last 20 years (INE 2012).

It has 261 km of coastline; 55 km faces the Mediterranean Sea and 216 km the Atlantic Ocean. The relief is diverse, mountains are in the Center and Northeast and large plains in the West that occupy 50% of the territory (Candau et al. 2002). The most dense and evergreen vegetation is presented in the Natural parks *Los Alcornocales*, *Del Estrecho* and *Sierra de las Nieves* that are also the zones with the highest NDVI values (Figure 4).

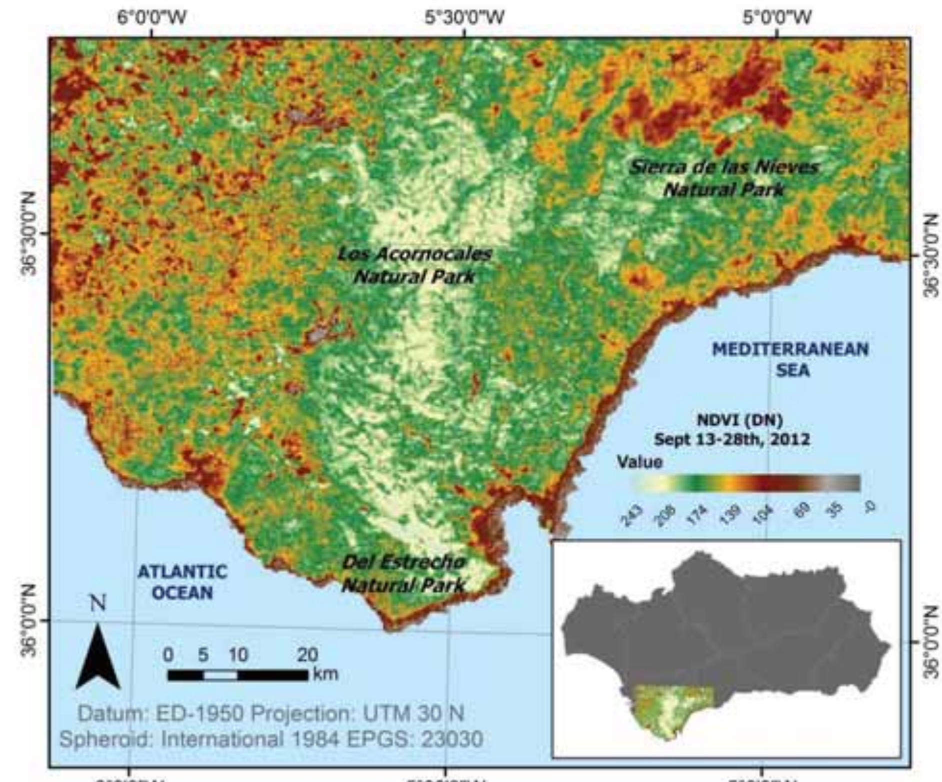

Figure 4. NDVI Map of the Study area. Values has been rescaled to digital numbers (DN).

The annual mean precipitation is 600 mm with 72% of humidity, the mean temperature in the warmest months, July and August, is 24-26 °C and higher than 10°C in the coldest months, December and January (Diputacion de Cadiz 2012).

Cadiz is characterized by high levels of biodiversity due to its contrasting topography, climate and geographical position. Also, it is an important biogeographic area of transit between Europe and Africa and is considered a strategic region for conservation of local and migratory species (Perez-Tris and Santos 2004, Diputacion de Cadiz 2012). Nevertheless, ecosystems are facing different biological and human pressures: the main threats are wildfire, aging of trees, poor natural regeneration, disease and pests. Also, low profit and lack on implementation of new technologies have led to poor management increasing degradation, desertification and land abandonment. Nowadays, areas without maintenance are more favorably for the establishment of bushes reducing open land species habitat (Moreno-Rueda and Pizarro 2007, Jordán López et al. 2008, Consejeria de Medio Ambiente 2010). Figure 5a exposes a visited area with bush encroachment in Cadiz. It is observed how annual vegetation is replaced by perennial vegetation which remains green during summer. The most frequent species found in this area are shown in Figure5b-e.

One of the main advantages of surveys in Andalusia is the availability of information. The Spanish legislation has ruled free access for data produced with public funds. The *Andalusian* government agency *Junta de Andalucía* has developed a website where plenty environmental and agricultural information is available. Its web portal offers historical climate data in raster format, links to visualize and download orthophotos, publications of environmental and climatic models, monitoring studies among others. Therein Cadiz was a convenient study area. The required input of this study had not only free access to the data but also high quality and low cost.

3.3 Fieldwork

Fieldwork was carried out from September 18th to September 27th 2012 in Cadiz Province (Andalusia, Spain). First, it was pursued to improve the understanding of Cadiz's ecosystems and dynamics related to encroachment as well as its contrasting geography. Secondly, its aim was to identify and collect bush encroaching species. Thirdly, it should help recognizing different covers and pixels with land cover change. Due to the extensive sampling effort to survey bush encroachment; access to areas and ground cover estimation, it was decided to use aerial images to detect areas with bush encroachment.

Figure 5. Pictures of encroahment in Cadiz .a. Areas with ongoing process of encroachment 21-Sep-2012. b-e Photos of the most dominant bushes species observed in the field. b. *Chamaerops humili-* **c.** *Rhamnus spp***. (saxatilis). d.** *Nerium oliander e***.** *Pistacia lentiscus*

Additionally, aerial images provided consistent information through time whereas fieldwork is only related to one date point. The method validation was performed using the same criteria. In summary, the work in the field provided a better comprehension of the study area and the local ecosystem conditions. Moreover, it contributed to an easier and faster analysis and appropriate interpretation of the aerial images and the landscape.

3.4 Data

3.4.1 Data Acquisition and Time Series Pre-processing

MODIS imagery was ordered from NASA Land Processes Distributed Active Archive Center (http://reverb.echo.nasa.gov). Images are gridded in Sinusoidal projection, WGS 84 datum and WGS 84 Spheroid. The imagery corresponds to MODIS/Terra Vegetation Indices 16-day 250m version 5 (MOD13Q1), from February 2000 to September 2012 (latest image available when the request was sent). The acquired images were clipped to the study area and stacked. The final data set was constrained to min.NDVI exclusively, it means all composites from July 28th to September 13th from 2001 to 2012 (36 composites in total).S

In order to work with NDVI time series, data was rescaled to digital numbers (DN) using Equation 2. The transformed data, now as DN from 0 to 255, was processed in TIMESAT 3.3 to fit, correct and recalculate the rescaled NDVI avoiding noise and outliers (de Bie et al. 2011, Srivastava 2011).

$$\textit{Equation } \mathbf{2}.$$

$$DN = 0.02125MVC - NDVI + 42.5$$

Where DN is Digital Numbers and MVC is Maximum Value Composite. The coefficients 0.02125 and 42.5 have been derived from MODIS provider parameters to rescale NDVI values to DN

3.4.2 Mask

Residential and agricultural areas were excluded from this study. These areas are under high human pressure; new constructions, irrigation systems, forestal harvesting among others generate abrupt changes that are out of this study scope. The ISODATA clustering classification (explained in section 3.5) was used to create an initial mask. Classes from 17 to 36 of the classified map from ISODATA were selected as classes of interest (Figure 6) because they group rangelands, forest and natural lands.

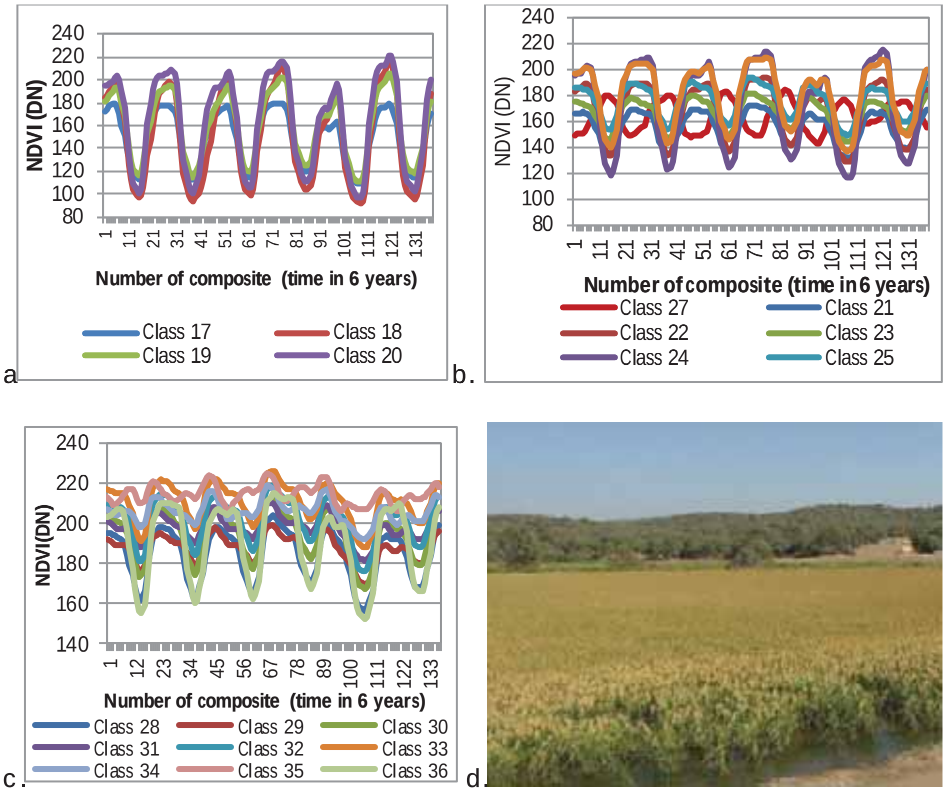

Figure 6. NDVI annual classes profiles (2001-2006). One composite is equivalent to 16 days a.From class 17 to 20. b. From class 21 to 27 c. From class 28 to 36. d Photo Class 27:Rice fields.

Class 27 are irrigated lands (Figure 6d), its trend is opposite to the regular NDVI patterns. It presents NDVI peaks in summer and valleys in winter (Figure 6b). Furthermore, Corine Land Cover 2006 from the European Environment Agency (EEA 2010) was used to improved and produce the final mask. The selected Corine land classes were Pastures (code: 231), Forest (code: 311, 312, 313), Shrub and/or herbaceous vegetation associations (code: 321, 322, 6323, 323). Figure 7a depicts the ISODATA classification map, the implemented mask is shown on Figure 7b while the masked study area is on Figure 7c.

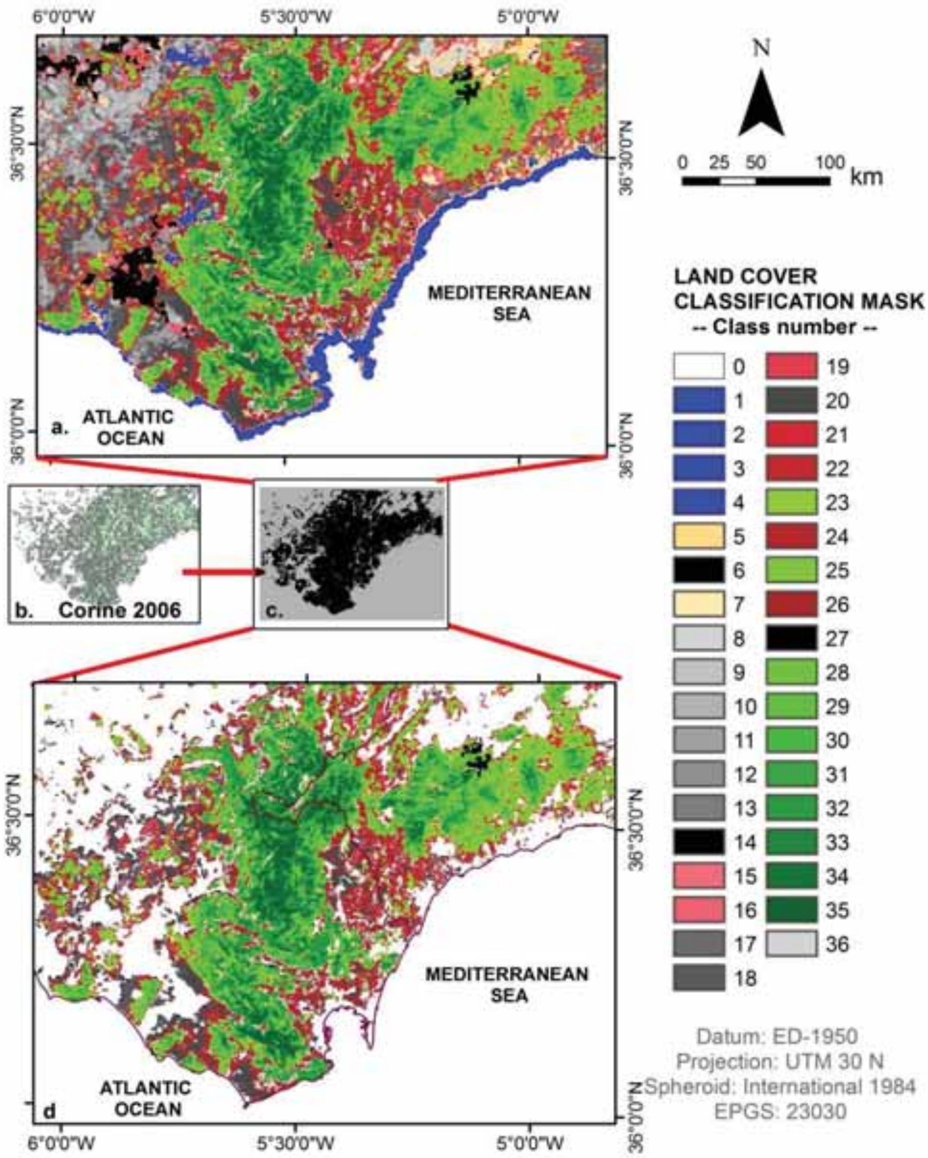

Figure 7. Land cover classes from ISODATA clustering a. Selected classification map after ISODTA clustering. b. Selected areas of Corine 2006 c. Mask combining ISODATA clustering and Corine 2006 d. Masked study area.

3.4.3 Aerial Images and Perennial Cover Estimation

This study focuses on the relationship between min.NDVI and perennial cover. Perennial cover estimation relied on aerial images visualization and interpretation. Imagery from different years and sources varied in resolution, color intensity, amount of light shadows and date. For that reason, the main criteria used to recognize perennial cover increase i.e. encroachment was the reduction of gaps among vegetation patches and notorious plant spreads in consecutive images. In Figure 8 is observed how the bottom of the pixel was cover by grass in 2003 and how perennial plants established in the next years (Figure 8). Although, the imagery dated from different months i.e. March, May and August, there was a clear difference between perennial and annual vegetation that is not affected by seasonality. It allowed a correct visual interpretation of the images and estimation of perennials.

Figure 8. Consecutive aerial images of pixels with encroachment.

Two independent imagery sources were used on the methods calibration and validation, thus the samples are independent:

- **Calibration:** Google™ earth imagery was used to identify Change and No-Change pixels in the study area. Digital Globe images of March or August 2003 (depending on the area), August 2005 and GeoEye imagery of July 2011 were surveyed. Identification of gradual changes in land cover through time was conducted observing Google™earth Historical imagery.
- **Validation:** Orthophotos available from *La Junta de Andalucia* website (http://www.juntadeandalucia.es/ medioambiente /site/rediam/portada/ visited in September, 2011) and Web Map Services-WMS were used to compound the validation dataset. Orthophotos were always taken in summer of 2001, 2006 and 2010 for the study area. The aerial images time comparison was done in ArcGIS 10.0.

For pixels in both data sets, perennial cover percentage was estimated based on a grid (5 x 5 cells with each cell 50 x 50m^2) cover (Figure 9). Each assessed pixel was divided in smaller squares that represent four percentage of the cell. The selected pixels with evergreen vegetation spread must demonstrate to be consistent through time (taking into account seasonal variations). In addition, shapefiles of *El Inventario Forestal Español* (Spanish Forestry Inventory-IFE 2006) and *Mapas de usos del suelo y coberturas vegetales* (Land Use and Vegetation Cover Map of Andalucia) 1:25.000 MUCVA 2007 were used to support the perennial cover estimation (Figure 10).

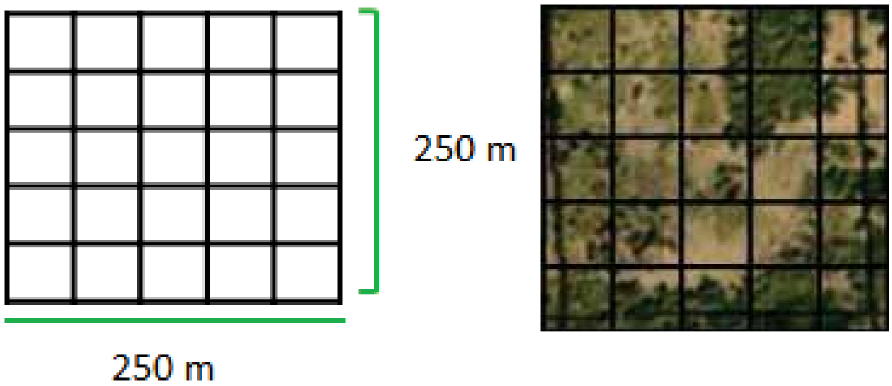

Figure 9. Grid used to estimate perennial cover. Left: Grid (5x5) b. Grid and pixel aerial image

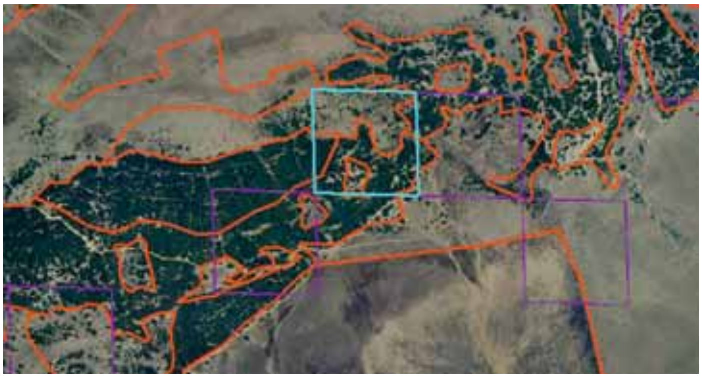

Figure 10. Vegetation vector-polygons files. Orange lines: Coverage from IFE (2006).

3.4.4 Calibration and Validation datasets

Purposive clustering sampling was carried out on this study. Due to the low rates of bush encroachment and the high anthropogenic influence in Cadiz, pixels selection was based on observation of aerial images for validation and calibration (Table 1, Appendix I). Pixels' min.NDVI profiles were generated in ERDAS IMAGINE 2011 and exported to Microsoft Excel 2010 and R 2.14.2 for further analysis

Because the three methods have different approaches, the calibration dataset was only used in Cover Fraction and QuantReg. CoverCAM calibration was supported by a reference time period. Cover-Fraction required solely the Change pixels group, whereas QuantReg worked with the complete calibration dataset The validation dataset was implemented in all methods to calculate Sensitivity, Specificity and PCC. Also, the impact of dry years was taken into consideration during the results analysis (Table 1).

Table 1. Calibration and Validation sets

	CALIBRATION			*VALIDATION*		
Aerial Images	**Google ™ earth**			**Orthophotos**		
	Year	*Annual Precipitation (mm)*		*Year*	*Annual Precipitation (mm)*	
	2003	1101		2001	844	
	2005	487		2006	711	
	2011	717		2010	1408	
Pixels Dataset	**Change n=17**	**No-Change n=17**	**Total n=34**	**Change n=17**	**No-Change n=35**	**Total n=52**
CoverCAM	No	No	No	Yes	Yes	Yes
Cover fraction	Yes	No	No	Yes	Yes	Yes
QuantReg	Yes	Yes	Yes	Yes	Yes	Yes

3.5 Change detection Methods

3.5.1 Method A: CoverCAM

3.5.1.1 Background

The Cover Composition Assessment Method (CoverCAM) has been developed in ITC and has been implemented in studies in Europe and Asia (Beltran-Abaunza 2009, Khan et al. 2010, de Bie et al. 2011, Srivastava 2011, Naemi 2012, Ali et al. 2013). The algorithm compares the area of interest at two different periods of time. The first one is a reference period which is assumed to be either constant or without any land cover change. Based on this assumption, the difference between the second period called monitoring period and the reference period is evaluated. Before any pre-processing both periods are defined by the researchers; the decision must be supported by the project objectives and the knowledge of the study area. The CoverCAM stepwise process was explained in detail by Srivastava (2011) and Ali et al. (2013 in press.) for NDVI SPOT (1km) in Andalusia (Figure 11, 12). The method is described in the following steps:

Reference period stepwise

1. *Selection of NDVI class map:* Unsupervised classification of the reference period runs repetitive for a range of classes (e.g. 10 to 50 on this research) in ERDAS IMAGINE 2011. The selection of the most appropriate number of classes is based on divergence statistics: average separability and minimum separability. The obtained classes are not spatially continuous; it means they are composed by several polygons which may have different climatic regimes, anthropogenic influence and other factors. Therefore, every polygon will be assessed as an independent unit in the monitoring period (Figure 11).

2. *Establishment of range tolerance:* The standard deviation (SD) of each NDVI class is calculated for each year of the reference period. To establish the range tolerance Pooled Standard Deviation (SDp) is computed from the obtained annual SD of the whole reference period. In general, it groups the SD of different years into one annual SD (Figure 11). The algorithm allows to assign weight (>1) to the SD, though the default value is 1.

Monitoring period stepwise

3. *Establishment of the tolerance range in every polygon*: The NDVI mean of each polygons is calculated for each year in the monitoring period. Then, the SDp (calculated from the reference period) is added to the mean NDVI in each independent polygon, delimitating their own tolerance range. Each NDVI value of each pixel (from the monitoring period) is evaluated and compared with its own tolerance range (Figure 12).

4. *Change detection:* The algorithm runs through the whole image and flags each pixel like a temporal change when the pixel's value fell outside its-own tolerance range. When the number of temporal change is higher than 66%, the change is significant. Polygons with just 2 pixels were excluded from this study for being considered no representative.

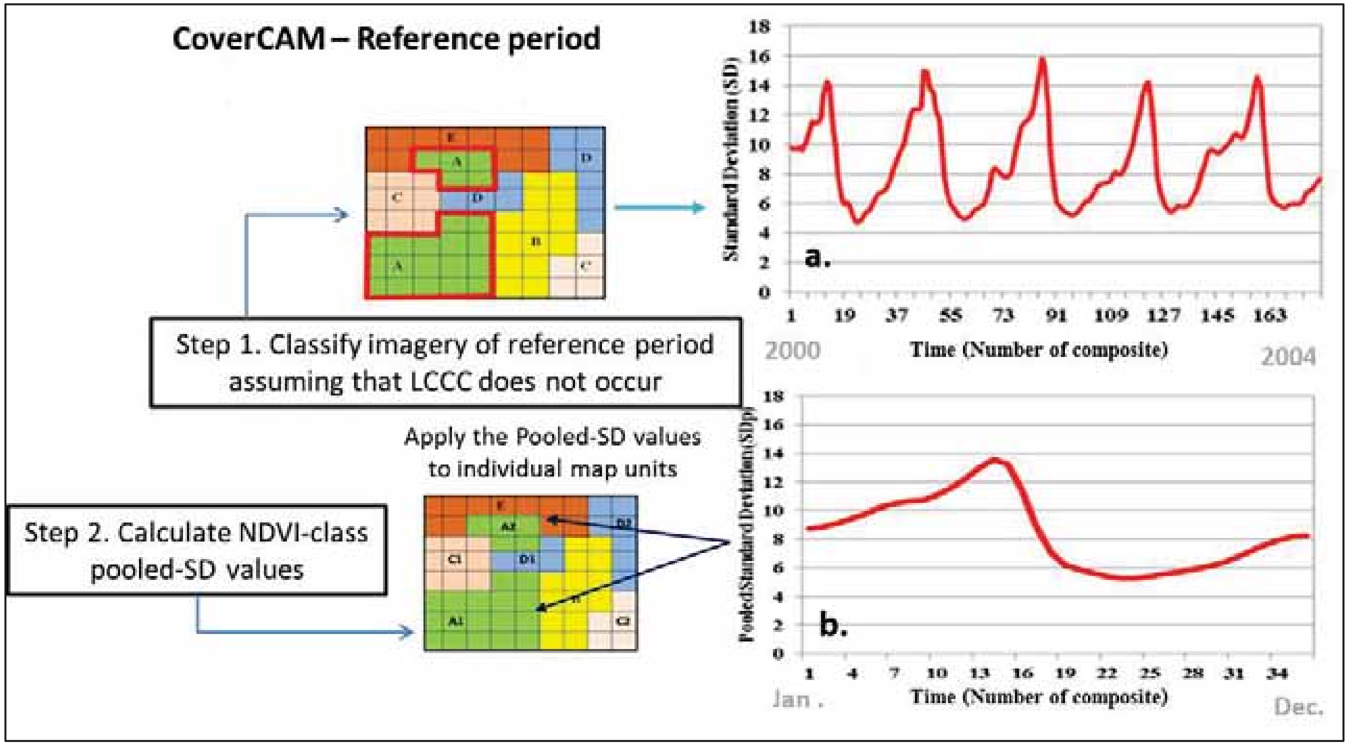

Figure 11. CoverCAM stepwise diagram for SPOT 1km, 10-days composite. a. Standard deviation (SD) of polygon A through the reference period (2000 to 2004). b. Pooled SD (SDp) of reference period: Annual mean of SD. LCCC= Land Cover Composition Change (Modified from Ali et al. 2013)

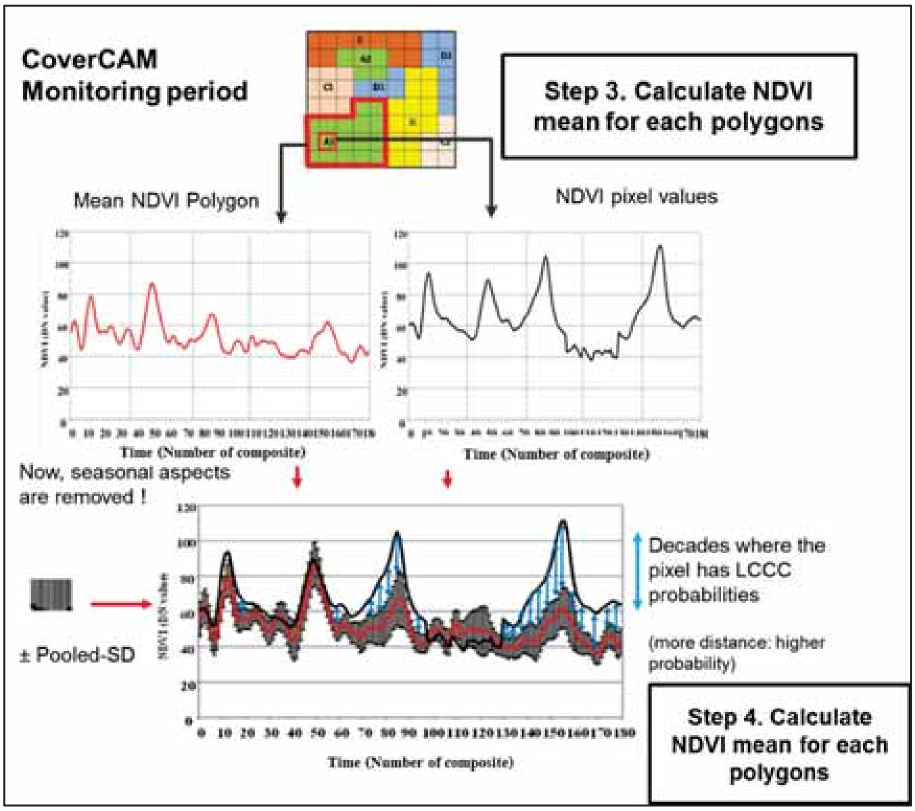

Figure 12. CoverCAM stepwise diagram of the monitoring period (2005-2010). LCCC= Land Cover Composition Change (Modified from Ali et al. 2013)

3.5.1.2 Justification

The CoverCAM prototype was designed to include spectral and temporal data from NDVI. It has been used widely for SPOT-Vegetation (1 km) and in less proportion for MODIS-NDVI (250m). CoverCAM has demonstrated to be appropriate in detection of abrupt changes. It has been successfully applied in (i) monitoring of flooded areas in Mozambique and water supplies in Iran (De Bie et al. 2008), (ii) improvement of crop calendar, land use and land cover maps (de Bie et al. 2011), (iii) solar plant construction and logged Eucalyptus trees in Andalusia (Srivastava 2011). One of the main advantages of CoverCAM is that it includes interannual variability from time series of NDVI, then it seeks anomalies due to land cover change but not caused by vegetation intrinsic dynamics.

Taking into consideration the strength of this approach, it was decided to combine CoverCAM with the min.NDVI criterion to drive the detection of bush encroachment in natural areas. But also we were aware of the user settings challenges as well as the choice of the reference and monitoring period.

3.5.1.3 CoverCAM Stepwise and Software

CoverCAM analysis for gradual cover change detection followed the stepwise process explained above in section 3.6.1. The input was min.NDVI MODIS 250m images from 2001 to 2012. The data has been rescaled previously to DN (Equation 2) in ordered to generate an image stack able to run in CoverCAM. The reference period was fixed from 2001 to 2006, and the monitoring period from 2007 to 2012, assigning equal number of years to both periods and aiming at including all interannual variability within the reference period. The selected SD was 1 and areas with less than 2 pixels were excluded because they were considered too small for the algorithm comparison. These settings were defined on the program interface (Figure 13).

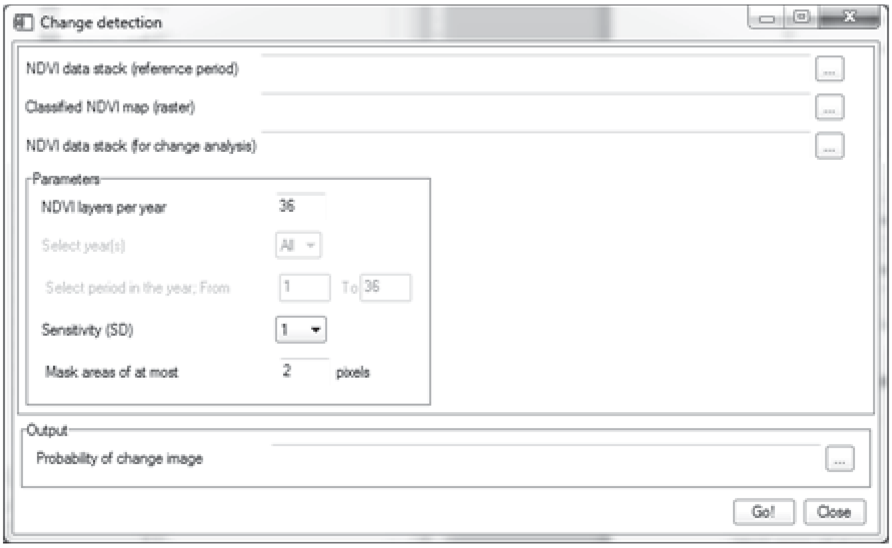

Figure 13. CoverCAM interface and user-settings

CoverCAM produced annual change probability maps from 2007 to 2012. The six maps were combined to generate the final probability change map. Each annual map was multiplied by a weight factor, with higher weight assigned to more recent years. The first year was multiplied by one, and the factor increased by one unit for each year. These factors pursued to enhance the most recent changes (Equation 3), and they have been implemented in previous CoverCAM studies (internal communication). The weighted maps were summed up to produce the final change map. The final change map was converted to polygons (shapefile) and transformed to UTM Projection Zone 30 North European, Datum 1950 (ED1950) and Spheroid International 1924 (ESPG: 22030) in ERDAS IMAGINE 2011.

$$\textit{Equation 3}$$

$$\textit{Pixel probability of Change} = 6 \times Map2012 + 5 \times Map2011 + 4 \times Map2010 + 3 \times Map2009 + 2 \times Map2008 + 1 \times Map2007$$

CoverCAM steps, from bullets 3 to 6, run on an Integrated Data Language prototype developed in ITC (Ali *et al,* 2013 in press).

Using Natural Breaks classification in ArcGIS 10.0, four categories of probability of accumulative change values were established. The categories are pixels with (*i*) significant min.NDVI increase or (*ii*) decrease and pixels with (*iii*) no significant increase or (iv) no significant decrease.

3.5.1.4 Evaluation

The validation dataset was used to assess PCC, Se and Sp of CoverCAM. The correct detection of CoverCAM was associated to Change pixels flag as "Pixels with significant min.NDVI increase". Similarly, No-Change pixels were classified correctly if they are flag as "Pixels with no significant increase or decrease". Alternatively to the validation dataset, 35 pixels with the highest probability of change (category *i*) were selected randomly to assess change CoverCAM detection accuracy. This was done because CoverCAM surveyed the whole study area and it was pursued to obtain information about its overall perfomancee in Cadiz.

3.5.2 Method B: Cover-Fraction

3.5.2.1 Background

NDVI values are directly related to vegetation cover density (Figure 13), vegetation type and seasonality. Figure 14a displays the summer NDVI profile of rangelands (class 19, 20), scrublands (class 23, 24, 25) and forest (class 33, 34, 35) from 2001 to 2006. The NDVI summer resulted likely convenient to differentiate among land cover classes. Even though overlaps among dense scrublands and forest occur. The mean summer NDVI for the whole study period (2001-2012) in grasslands is 90 DN (n=12 σ=13.8), this being class the easiest to recognize. Differences among the other two classes are less clear. Scrublands' mean summer NDVI is 153 DN (n=7 σ=10.4) and forest's summer NDVI is 168 DN (n=7 σ=11.5). The summer NDVI mean values for the three classes differed. However, their SD overlapped marking the influence of plant diversity and abiotic variables no considered.

3.5.2.2 Justification

Vegetation type and cover density have demonstrated to be relevant to study NDVI and cover composition change (Geerken 2009, Oldeland et al. 2010). Because of that, three main land cover classes were fixed:

- Rangelands/grasslands: It is covered by annual vegetation including herbs, grass and bare soil. It does not have any or very sparse (<5%) perennial vegetation. During summer, it has null or very low photosynthetic activity (Figure 14b, Class 5, 7).
- Scrublands: It is a mixed cover of annual and perennial vegetation, evergreen bushes and trees with grass. Its vegetation density goes from sparse to very dense (5% to 90%). These areas are candidates for encroachment (Figure 14c, Class 23, 25, 28).
- Forest: It is forested areas completely covered by evergreen plants (>90%), their interannual NDVI variance is relatively low and are not suitable for encroachment (Figure 14b, Class 33, 34, 35).

3.5.2.3 Cover-Fraction Stepwise and Software

This research aimed to find pixels with bush encroachment. Therefore, this method was focused exclusively on Change pixels, from the calibration dataset, to establish a linear equation that estimates perennial cover from min.NDVI. Initially, linear regression assumptions were considered. It was demonstrated that the min.NDVI calibration dataset for Change pixels fulfill all linear relation assumptions (Table 2). Firstly, the linearity assumption was accepted using Lack of Fit Test with α=0.05 and p=0.921 (Trexler et al. 1988). Secondly, residual plots were elaborated to explore their distribution. Figure 15a shows a consistent spread of the residuals and Figure 15b shows how the points of the predicted and the observed cumulative proportions clustered to the square regression line. The Breush-Pagan test was performed to state homocedasticity with statistical significance; α=0.05 and p=0.921 (Breusch and Pagan 1979). Thirdly, the Durbin-Watson (DB=1.74) statistic was calculated to accept the assumption of independence of errors (Durbin and Watson 1971, Quinn and Keough 2005). Finally, to test normality of the residuals the Shapiro-Wilk statistic was calculated (SW=0.98) (Royston 1995, Quinn and Keough 2005). In short, the sample satisfies all the assumptions to test the linear regression between Change pixels and perennial cover.

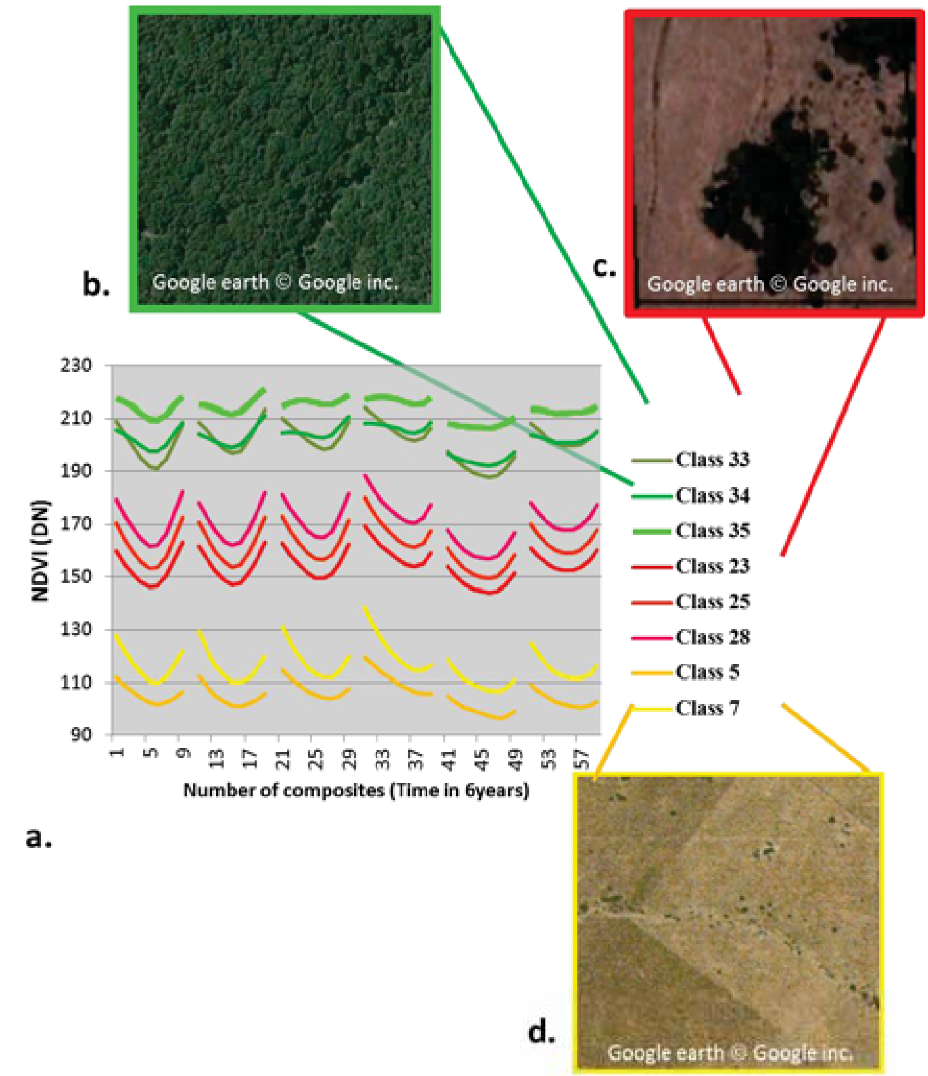

Figure 14. Summer NDVI-profiles and imagery of vegetation classes obtained from ISODATA classification. a. Rangelands/Grasslands b. Scrublands c. Summer NDVI profiles d. Forest

The statistical analysis was carried out in IBM SPSS Statistics 21 and R 2.14.2.

Table 2. Linear assumption test of Calibration dataset. d.f: degrees of freedom. F: Fisher statistics

Test	Hypothesis		
Lack of Fit Test	*Ho: A linear model is appropriate*		
d.f.	**F**	***p*- test**	**Decision**
36 , 13	0.55	0.92	Ho cannot be rejected
Stunderized Breush-Pagan Test	*Ho: The errors have the same variance*		
d.f.	**Stat.**	***p*- test**	**Decision**
1	1.98	0.16	Ho cannot be rejected
Durbin-Watson Statistic	Residuals correlation measurement: Durbin – Watson statistics ranges from 0 to 4		
Residuals are not correlated if the statistic falls within 1.5-2.5	D-B = 1.74		Residuals are not correlated
Shapiro Wilk test	*Ho: The distribution of the residuals is normal*		
d.f.	**Stat.**	***p*- test**	**Decision**
51	0.98	0.72	Ho cannot be rejected

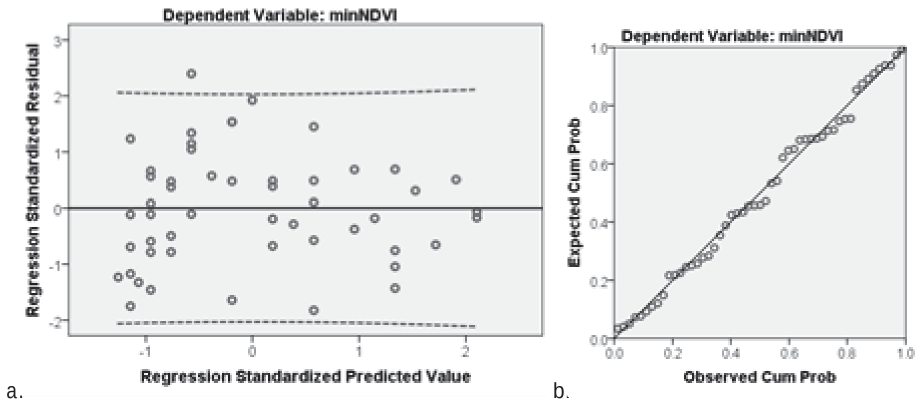

Figure 15. Scatterplot of variance of residuals a. Relation between the residuals (or errors) and the predicted value; solid line: fit line; dotted lines represent 95% interval confidence. b. Probability plots (P -P plots). Cum Prob: Cumulative Probability

The linear regression between min.NDVI values and perennial cover was computed to establish the equation that predicts perennial cover from min.NDVI. The used min.NDVI is from 2002, 2005 and 2011. It must be the same that aerial images date to be comparable.

3.5.2.4 Evaluation

The calibration dataset was used to predict perennial cover from 2001, 2006 and 2010 min.NDVI. These years were chosen because availability of Orthophotos.

To assess bush encroachment detection by Cover-Fraction, the difference between 2001 and 2010 perennial cover was calculated from predicted values which are obtained from the perennial cover of the evaluation dataset. No-Change pixels have 0% observed cover change, from the imagery visualization, and it was expected them to have low or null perennial cover change when the difference between predicted cover was computed.

In the same way, it was expected that predicted perennial cover of Change pixels differ significantly when 2001 and 2010 estimated cover were compared. Change in cover was considered significant when the difference between 2001 and 2010 estimated covers fall outside the 95% confidence level. Total accuracy, sensitivity and specificity were computed. Also, the correlation of observed against estimated perennial cover was calculated (R^2).

3.5.3 Method C: QuantReg

3.5.3.1 Background

Quantile regression is a statistical method developed by Koenker and Bassett (1978) which focuses on the comparison of the variable response through this own gradient. Cade and Noon (2003) explains it as a method that "estimates multiple rate of change (slopes) from the minimum to the maximum response variable". It is a semiparametric test because it assumes non-Gaussian error distribution but uses a parametric form to determine the model parameters, e.g. $\beta_0X_0 + \beta_1X_1$. In ecology, it has been demonstrated to be very convenient when not all variables can be measured or are included in the research. Sankaran et al. (2005), applying linear QuantReg, exposed how woody canopy closure is constrained by rainfall in African savannas with less than 650mm mean annual precipitation. Encroachment in savannas with higher mean annual precipitation is controlled by fire, herbivory or other disturbances.

3.5.3.2 Justification

The global mean NDVI profile of the study area (Figure 16) depicts the intearannual NDVI variation which follows the annual climatic conditions. For example in 2005 Spain suffered a very extreme drought (Figure 17a), and in 2012 temperatures reached 50°C, demonstrating the strength of the summers for these years, patterns that were also observed in the NDVI profile. Conversely, 2010 was a very humid years (Figure 17b). Despite this patterns, there is not a significant correlation between mean min.NDVI and precipitation (R^2=0.48).

The plausible effect of dry years in encroachment detection was observed when pixels profiles were analyzed (Figure 18). The min.NDVI trend exceled the NDVI drops that match with the driest years, i.e. 2005, 2009 and 2012. Herein, QuantReg was proposed to detect encroachment, considering the impact of climate when min.NDVI and time are the only assessed variables.

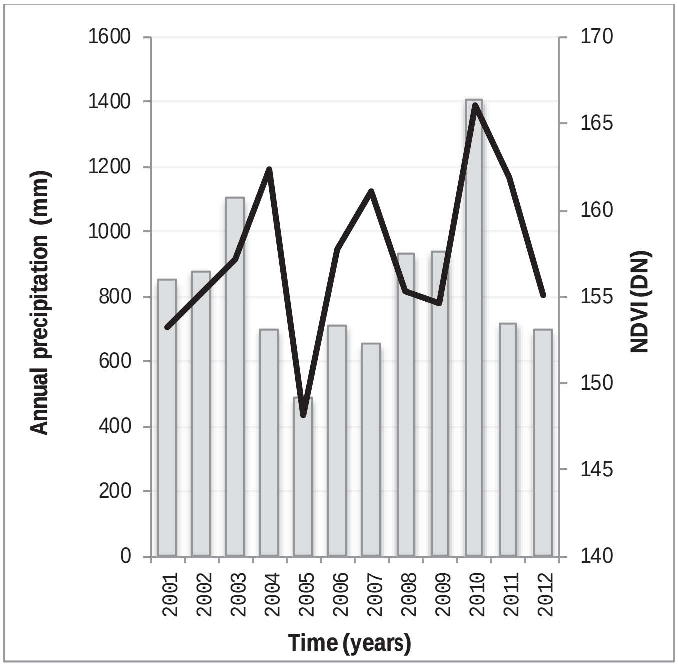

Figure 16. Annual precipitation and annual min.NDVI of the study area. mm= millimeters. DN= Digital Numbers

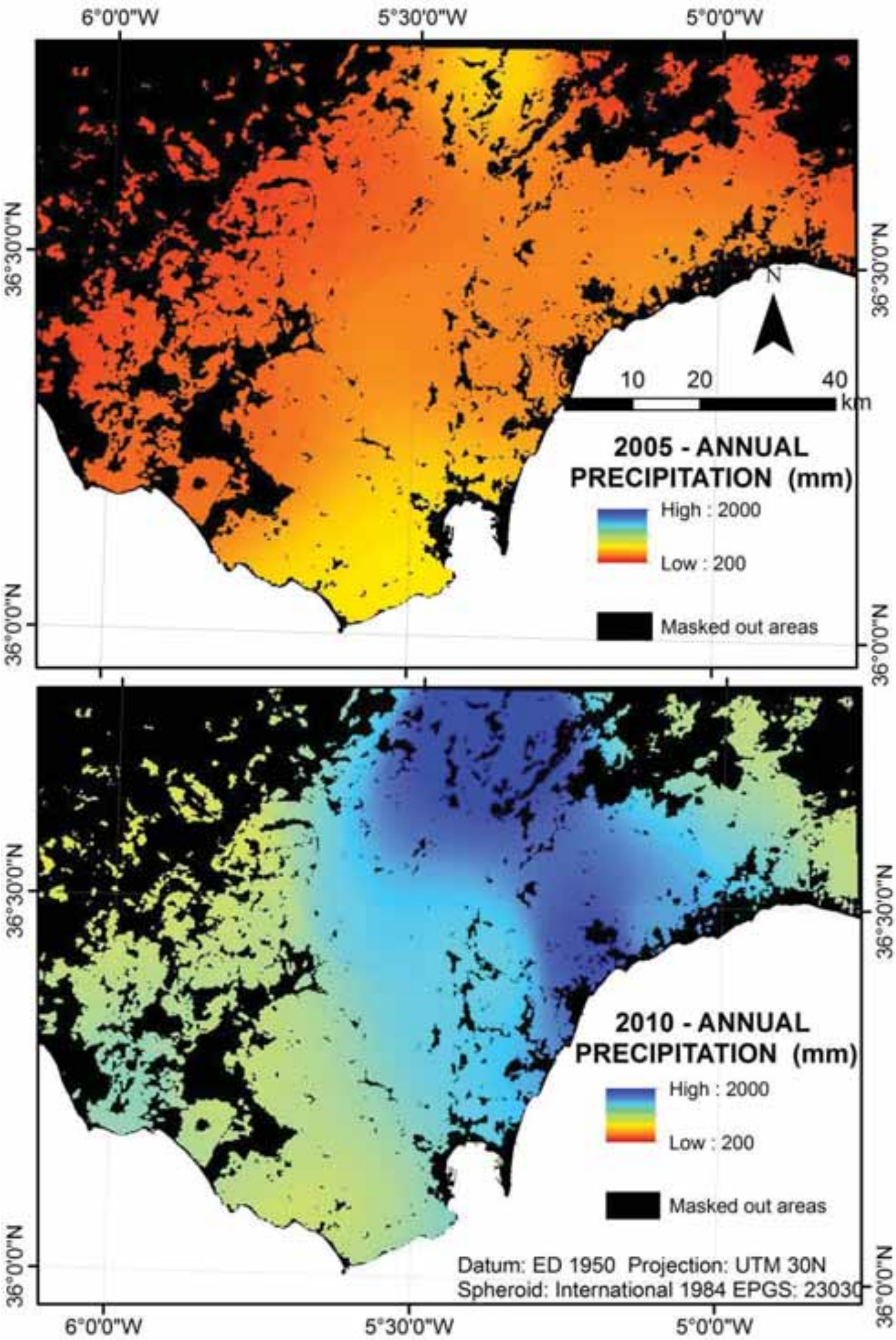

Figure 17. Annual precipitation of the study area. a. 2005: The driest year in the study period. b. The most humid year In the study period. Black areas where masked out.

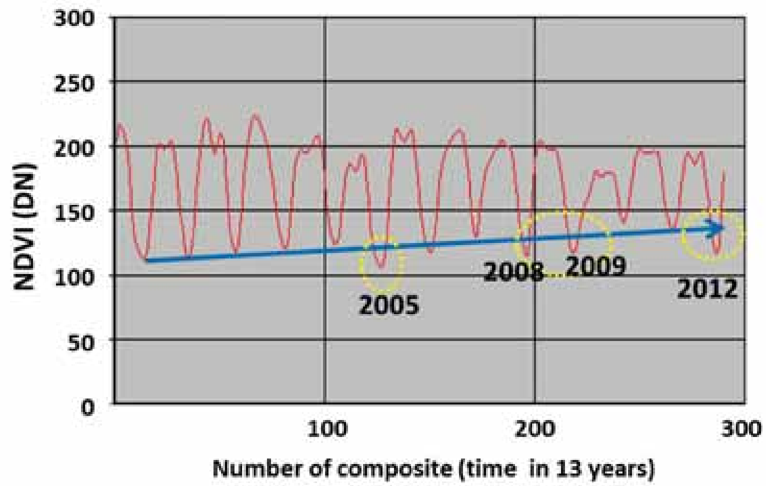

Figure 18. NDVI profile of pixel with encroachment from 2000 to 2012. One composite is 16 days.

3.5.3.3 QuantReg Stepwise and Software

An algorithm to compare the performance of min.NDVI in five quantiles was developed in R 2.14.2, implementing 'QuantReg' R package designed by Koenker (2006) The linear QuantReg ran for the 0.25, 0.33, 0.5, 0.66 and 0.75 for each pixel. 0.25, 0.5 and 0.75 are the most used quantiles in data analysis. In addition, the quantiles 0.33 and 0.66 were selected because they are equivalent to the number of records in 3 and 6 years (9 and 18 NDVI composites respectively).

In this method, the complete calibration dataset was used. Two groups of pixels 17 with Change and 17 with No-Change were assessed. The slope, intercept, *t-value* and *p-value* of each pixel were obtained through the Linear QuantReg algorithm. A significant slope was associated with bush encroachment. The slope analysis was performed by pixel and within the five different quantiles. The null hypothesis is described in Table 3.

To evaluate differences among quantiles within the same group, the ANOVA test was used (Koenker 2006). Additionally, to evaluate difference among group, the Kruskal –Wallis non parametric test was used, hypothesis are explained in Table 3. Both statistical analysis were carried out in R 2.14.2. Quantiles that showed a significant difference between Change and No-Change pixels were selected for the validation.

Table 3. QuantReg hypothesis

Slope significance. Student test was implemented to assess each pixel through all quantiles
$\boldsymbol{H_o}$**:** $\beta_1=0$ $\boldsymbol{H_a}$: $\beta_1 \neq 0$ where β_1 is the slope The $\mathbf{H_o}$ is rejected with an $\alpha=0.05$ ($p<0.05$)
Difference within quantiles: ANOVA test was used to compare if all quantiles perform similarly. First, it was run for Change and afterwards for No-Change pixels
$\boldsymbol{H_o}$**:** p-value$_{0.25}$ = p-value$_{0.33}$ =p-value $_{0.5}$ = p-value $_{0.66}$= p-value $_{0.75}$ $\boldsymbol{H_a}$: *At least one quartile has p-values significantly different from the others* *Where p-value is the slope significance* *The* $\boldsymbol{H_o}$ *is rejected with an* $\alpha=0.05$ ($p<0.05$)
Difference between pixels groups : Kruskal-Wallis test was used to compare between Change and No-Change pixels within each quantile
$\boldsymbol{H_o}$**:** *Change p-value*$_{[j]}$ = *No-Change p-value*$_{[j]}$ $\boldsymbol{H_a}$: *Change p-value*$_{[j]}$ ≠ *No-Change p-value*$_{[j]}$ *Where p-value is the slope significance* *j is 0.25, 0.33, 0.5, 0.66, 0.75 quantiles* *The* $\boldsymbol{H_o}$ *is rejected with an* $\alpha=0.05$ ($p<0.05$)

3.5.3.4 Evaluation

The validation dataset was used to evaluate QuantReg performance. PCC, Se and Sp were calculated for the significant quantiles. Pixels with significant slope at α=0.05 were flagged pixels with change and pixels with no significant slope were flagged as no change pixels.

Chapter 4. Results

4.1 Method A: CoverCAM

4.1.1 Calibration

The classified map with 36 classes was selected from ISODATA clustering as the most appropriate. This decision was supported by divergence statistics; minimum separability and average separability which are measurements of the difference among classes (Beltran-Abaunza 2009, de Bie et al. 2011, Nguyen et al. 2011, Srivastava 2011, Naemi 2012). Figure 19 shows a peak in average separability and a constant value in minimum separability for 36 classes which also was suitable taking into consideration the small size of the study area. Initially it was pursued to find a peak in both to select the best map but it did not occur.

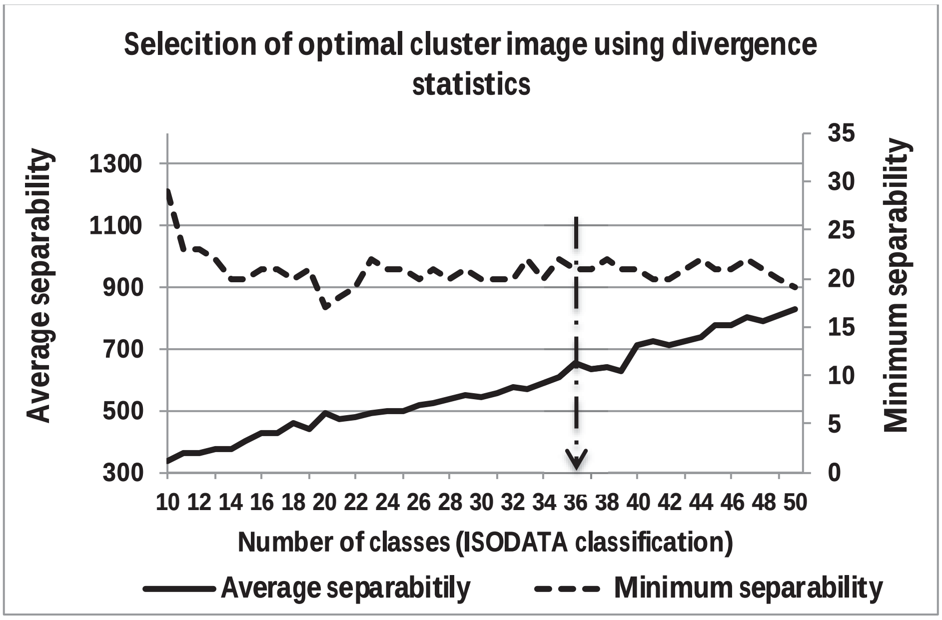

Figure 19. Divergence statistics plot from ISODATA clustering

CoverCAM had a high detection of areas with abrupt changes e.g. dam construction and, solar panels (Appendix I). Alterations caused by humans, transformed the ecosystem, thus properties pronouncing changes on the pixel profiles. Figure 20 shows an area before and after flooding caused by dam expansion. Figure 20a and 20b pointed that the event must have occurred between summer of 2007 and 2010. Further, looking at the whole annual pixel profile from 2000 to 2012, it was concluded that the cover change started in summer 2009 and the surface was flooded in 2010 (Figure 19c).

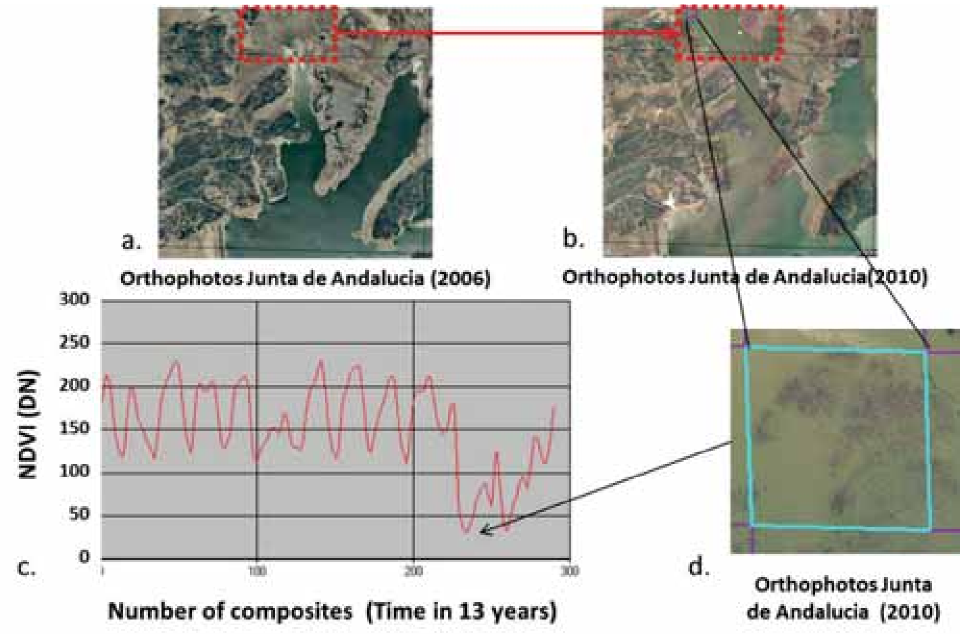

Figure 20. Pixels with abrupt change. a. Area before dam expansion 2007 b. Area after dam expansion 2010. c NDVI profile from one flooded pixel. d. Zoom into a flooded pixel. Red dotted squares emphasized the affected area

The resulted probability of change accumulative values ranges from -1905 to 3074 (not normalized scale). Negative values were associated with loss of vegetation cover while positive changes were related to vegetation increase (Figure 21). The class with the highes probability of min.NDVI increase is the most relevant class in this survey and it has 103 pixels a magnitude of change that ranges from 276 to 3074. It was likely that this class flagged pixels with bush encroachment. In the same way, a high probability of min.NDVI decrease should point out pixels that have lost vegetation cover. This class includes 90 pixels between – 1905 and – 276 magnitude of change. The other classes were flagged like no significant change and group the majority of the pixels which are expected to have a constant vegetation cover through time.

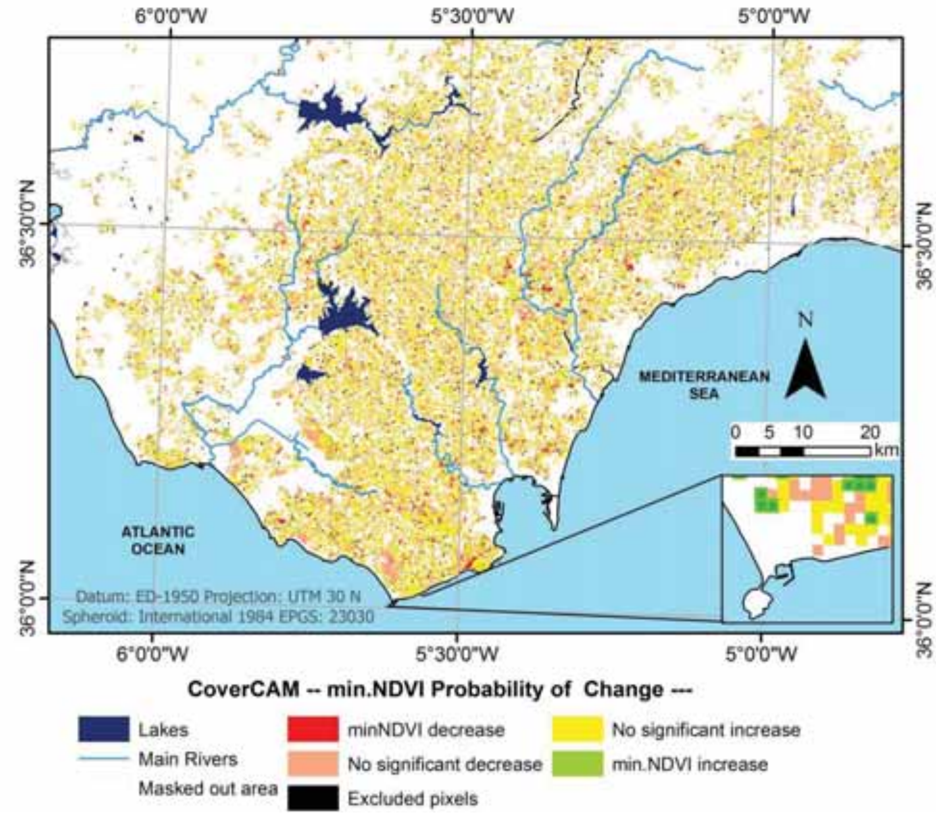

Figure 21. Probability of change map produced by CoverCAM.

4.1.2 Validation

After the validation dataset was implemented, it was found that CoverCAM had very low detection of pixels with Change (*Se*=12%), No-Change pixels were correctly classified (100%) which improved the method PCC=0.71 and brought out an overestimation of CoverCAM performance. It is relevant to recapitulate that the study's main objective was to detect pixels with perennial cover increase. Therefore it is valid to affirm that CoverCAM is not able to recognize bush encroachment. Additionally, when pixels flagged with high probability of min.NDVI were surveyed (n=35, random selection Appendix I), a low bush encroachment detection was also found (41%).

Otherwise, pixels highlighted with significant min.NDVI decrease were highly correlated with loss of vegetation cover; built ups, golf fields, solar panels construction and amongst others (Appendix I). In summary, CoverCAM conserves its high detection of abrupt changes but does not work for bush encroachment (Appendix I).

4.2 Method B: Cover-Fraction

4.2.1 Calibration

Equation 4 describes the linear regression between min.NDVI and perennial cover (Figure 22). The correlation coefficient was R^2=0.803 and the slope (β_1=0.7938) was significant with α=0.05. The obtained equation was used to estimate perennial cover and to identify pixels with bush encroachment. 51 values were used to estimate perennial cover. They were obtained from the survey of 17 pixels at three different times 2003, 2006 and 2011.

Equation 4.

$$F_{(Min.NDVI)} = 0.793 PerennialCover + 108.18$$

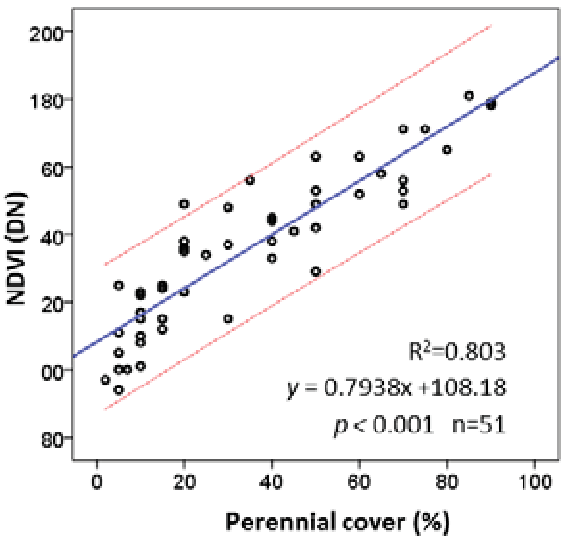

Figure 22. Cover Fraction Linear regression. Blue line: linear regression. Red line: Confidence interval 95%

4.2.2 Validation

The correlation between observed and predicted perennial cover by Cover Fraction is R^2=0.56 (n=156; Figure 23a). When Change and No-Change pixels were evaluated separately (Figure 23b), it was revealed that No-Change pixels are more accurately estimated (R^2=0.62 n=105) than Change pixels (R^2=0.42

n=51). These results were contradictory because the Cover Fraction equation was obtained from a dataset that included only min.NDVI values of Change pixels.

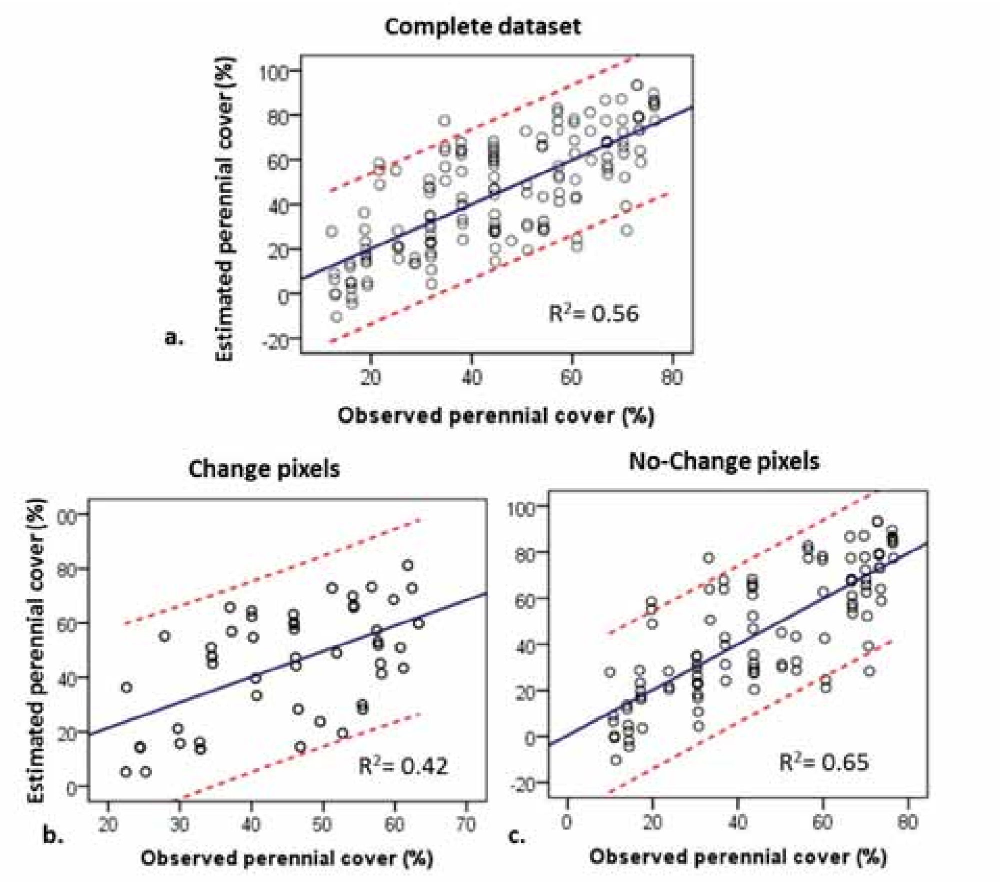

Figure 23. Estimated versus observed perennial cover by Cover Fraction. a. Correlation of the complete dataset. b. Left: correlation of Change pixels Right: Correlation of No-Change pixels. Solid line is the linear regression and dotted lines is 95% confidence level

The detection of pixels with bush encroachment was based on perennial cover change. Perennial cover was predicted from Equation 4, if the difference between perennial covers during the study period (2001-2011) was higher than ± 6.45 DN (95 % confidence level). In this case, pixels were considered as Change pixels, otherwise as No-Change pixels. The method's PCC was 0.52. Cover-Fraction prediction of Change pixels was *Se*=0.65 and had a low prediction of No-Change pixels *Sp*=0.22. It was found that the method overestimates perennial cover in No-Change pixels.

4.3 Method C: QuantReg

4.3.1 Calibration

Figure 24 shows the outcomes of the QuantReg for Change and No-Change pixels (Appendix II). It is observed that linear regression trends are similar in Change pixels across all quantiles. By contrast, No-Change pixels present significant linear regression in the upper quantiles (0.66, 0.75), but not in the lower quantiles (0.25, 0.33, 0.5). The difference of *p-values* within quantiles for the same pixel groups, i.e. Change or No-Change pixel group, was assessed with ANOVA. The *p-values* distribution of QuantReg is homogeneous in Change (p=0.2479 n=17) pixels but is significantly heterogeneous in No-Change pixels (p=0.0041 n=17).

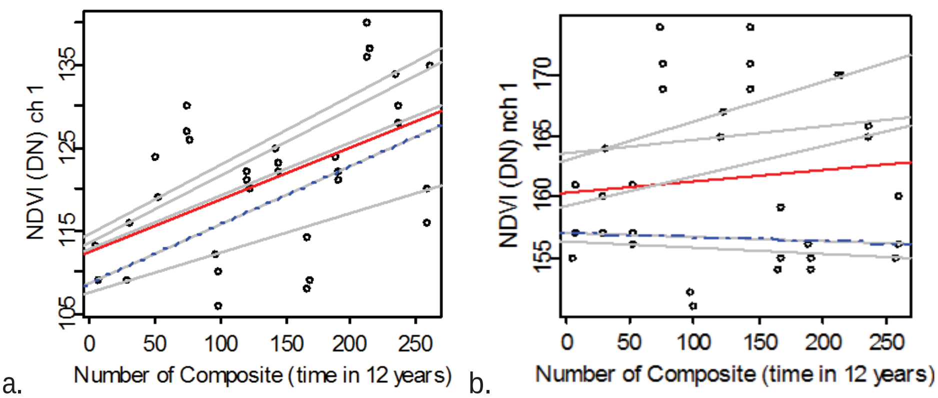

Figure 24. QuantReg plots. a. Change pixel b. No-Change pixel. The red line is the standard linear regression. The blue dotted line is the 0.33 QuantReg and the gray lines are the other quantiles regressions.

The distribution and significance of the *p-values* for Change and No-Change pixels is displayed in Figure 25. The lower quantiles 0.25, 0.33 and 0.5 are the most informative; *p-values* from change pixels mainly cluster between 0 and 0.05 while No-Change pixels have a wide spread frequently above 0.1. The quantiles 0.66 and 0.75 have a similar pattern in both groups.

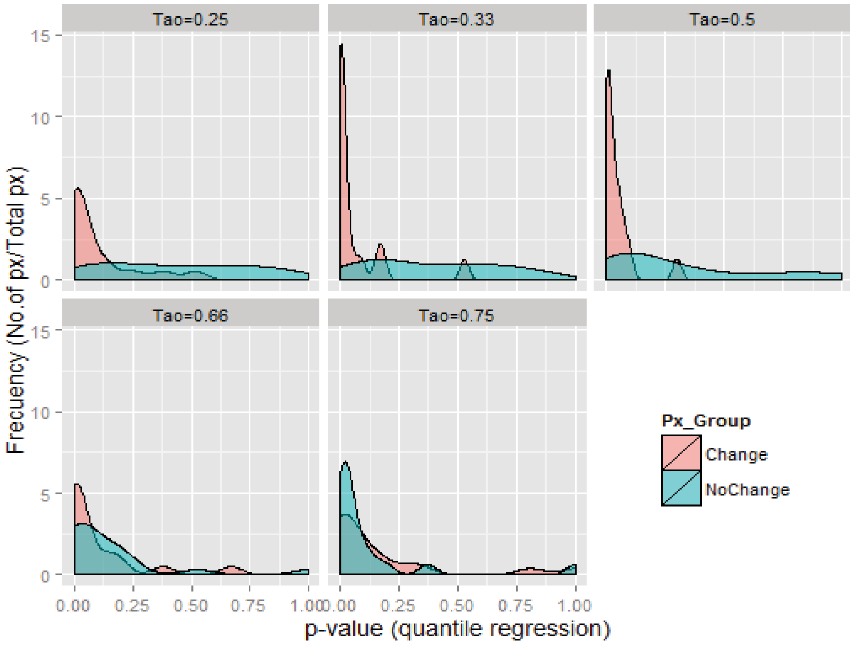

Figure 25. Frequency of QuantReg p-values of Change and No-Change pixels under different quantiles.

4.3.2 Validation

Comparisons between Change and No-Change pixels within the same Quantile demonstrated significant differences for 0.25, 0.33 and 0.5 quantiles with an α=0.05 (Table 4). For that reason, the Quantiles 0.25, 0.33 and 0.5 were used during the method validation. PCC, Se and Sp were calculated. The methods with the highest PCC and Se are the linear regression of the 0.33 and 0.5 quantiles (Table 4). In general, the three evaluated quantiles had higher Sp than Se.

Table 4. QuantReg comparison of *p-values*.of assessed quantiles

Quantile	*Kruskal Wallis Test*	*Decision*	*Conclusion*
0.25	0.00018	Reject *Ho*	There is a significant difference between Change and No-Change pixels
0.33	0.00007	Reject *Ho*	There is a significant difference between Change and No-Change pixels
0.50	0.00061	Reject *Ho*	There is a significant difference between Change and No-Change pixels
0.66	0.24850	Accept *Ho*	There is a not a significant difference between Change and No-Change pixels
0.75	0.86320	Accept *Ho*	There is not a significant difference between Change and No-Change pixels

4.4 Summary of the Methods Performance

Three indexes from the confusion matrix were calculated to assess and compare the methods performance (Table 5). PCC provides a general idea of the methods results; however, it must be carefully analyzed to avoid misinterpretations of the methods detection power because is highly affected by the correct prediction of No-Change pixels. This study pursued to highlight Change pixels, specifically pixels with bush encroachment, and it was not interested in No-Change pixels which are the majority. For that reason, Sensitivity was the main criterion to evaluate the method's performance. It informs about how many Change pixels were correctly predicted by each method. In this way, QuantReg of 0.33 and 0.5 quantiles are the methods that provide significant results with 0.71 and 0.82 Sensitivity, respectively. Their total accuracy is 0.77 which demonstrated also their power to classify correctly No-Change pixels. The other methods, CoverCAM, Cover Fraction and Linear regression for the other quantiles are not capable to detect pixels with bush encroachment. The summary of the methods is on Table 6.

Table 5. Accuracy measures of the methods

	CoverCAM	*Cover Fraction*	*QuantReg*		
			0.25	**0.33**	**0.5**
PCC	0.71	0.52	0.63	**0.77**	**0.77**
Sensitivity	0.12	0.65	0.41	0.71	**0.82**
Specificity	1	0.46	0.74	**0.80**	0.74

Table 6. Three methods comparative table

	Calibration	Output	Validation (criteria)	Additional performance criteria	Research decisions	Advantages	Disadvantages
CoverCAM (Method A)	Reference period	• Change map with change values (Not normalized range)	Change and No-Change dataset • PCC • Sensitivity • Specificity	Random sample of pixels with 35 highest change values	• Reference and Monitoring period length • Change threshold (1SD) • Classification change categories (natural breaks)	• It includes interannual variability • It runs for large areas • It generates a Change map • It detects abrupt changes	• It is not able to capture gradual changes • Results accuracy depend on choice user-settings
Cover-Fraction (Method B)	Change pixels	• Equation to Estimate perennial cover (%cover)	Change and No-Change dataset • PCC • Sensitivity • Specificity	Comparison of predicted vs. observed perennial cover (R^2)	Change higher than 95% confidence interval is considered as significant Change	• It is fast to operate • It brings out information about change in cover magnitudes (%)	• It requires training data set to find the equation • Highly affected by interannual climatic variation • Data selection is forced by aerial images availability • Perennial cover estimation decreased precision
QuantReg (Method C)	Change and No-Change pixels	• Slope significance (p-values)	Change and No-Change dataset • PCC • Sensitivity • Specificity	No	Data analysis was tested with α=0.05: • QuantReg slope p-value • Difference among quantiles • Difference between Change and No-Change pixels	• It is very robust to interannual climatic variation • Its detection is based on though time NDVI • Bush encroachment is significant detected	• An algorithm must be developed to perform studies at regional scale • Magnitude of change is not included in the output

Chapter 5. Discussion

This research explored the potential of min.NDVI time series to detect bush encroachment. Taking advantage of data periodicity but being aware of its moderate spatial resolution (250m), it is achieved to establish NDVI trends in Change pixels that are not observed in No-Change pixels. This difference between trends is enhanced after the NDVI annual profile is constrained to the novel approach of min.NDVI. In fact, min.NDVI only represented the greenness of perennial vegetation while annual plants are dried out, dead or have turned into hay. It is remarkable that the 3 composites of min.NDVI are from the driest and warmest period of the year. Also, the meaningfulness of the data series has been shown. This finding is coherent with other studies where coarse spatial resolution imagery is compensated by hyper temporal data (Stellmes et al. 2010).

This study explains the potential of QuantReg, a method that uses free access data and it does not require extensive resources as other surveys in large areas. The findings show a significant performance of QuantReg which provides a robust approach to develop an algorithm for bush encroachment detection. The other two methods, CoverCAM and Cover-Fraction, show low detection. All evaluated methods are based on min.NDVI which enhances the difference between perennial and annual vegetation.

5.1 CoverCAM Performance

CoverCAM detection of abrupt changes such as flooding, deforestation, logging, solar panels construction has been proven in previous studies (De Bie et al. 2008, Srivastava 2011). In spite of this, it shows a low detection power to flag bush encroachment in Cadiz. The weight assigned to the annual probability change maps (2007 to 2012) and the applied default threshold (1SD) are potential reasons to explain its low bush encroachment detection. Naemi (2012) described the important role of user-settings choice. She demonstrated how land cover change is underestimated by increasing the threshold (> 2SD), alternatively a low threshold leads to overestimation. Additionally, the classified NDVI map selection from ISODATA clustering has been robustly supported by divergence statistics. De Bie et al. (2008) and Khan et al. (2010) obtained notorious peaks of minimum and maximum statistics using SPOT-Vegetation 1 km^2 , as Ali et al. (2013) did for NDVI-MODIS 250m. Despite of this, the divergence statistics results in Cadiz reveal less discrepancy within the number of classes (Figure 19) impeding a solid classification map choice. The absence of a consistent peak for both, minimum and maximum separability may have a negative impact in CoverCAM performance. One of the plausible reasons of this is the high fragmentation of the Cadiz landscape and anthropogenic pressure.

CoverCAM has been widely implemented for the analysis of complete NDVI annual profiles. The selection of 3 composites for each year could reduce the power detection of CoverCAM. All possible reasons for its low bush encroachment detection should be tested in further studies. For that purpose, tuning of the user-settings (length of reference and monitoring periods, threshold SD) and the weight of change probability map must be considered.

5.2 Cover-Fraction Performance

It was found that the Cover Fraction equation underestimates perennial cover of Change-pixels reducing bush encroachment detection, at the same time overestimating the cover of No-Change pixels. In sum, the Cover-Fraction method has the lowest PCC of all methods. The analysis of the relationship between NDVI global means and precipitation (Figure 16) revealed that the calibration data set includes the lowest NDVI values from the whole study period (2005) and in general dry years (Table 1). In comparison, the validation dataset was constituted by humid years and hold the NDVI peak (2010) from 2001 to 2012. This difference in rainfall has a negative impact in the perennial cover equation.

The correlation between perennial cover and min.NDVI is significant in the calibration dataset. However, the validation dataset show a low performance of this method. In addition, Change pixels are frequently classified without change while No-Change pixels are flagged as pixels with perennial increase. This result is unexpected because the equation was estimated exclusively from the bush encroachment pixels dataset (Figure 22). Explanations for this low R^2 during the method validation could be derived from:

- Estimation of perennial cover: Visualization of images through time and a grid were used to estimate perennial cover. Implementation of segmentation software like eCognition may increase the precision of perennial estimation.
- Linear regression approach: Linear regression is the most used method to assess relationships between variables (Cade and Noon 2003) and the Cover-Fraction dataset appeared to be robust for this methods because it fulfilled all the assumptions. However, its performance is poor during the validation. The next step could be the

implementation of more complex mathematical functions which have been used in studies of ecology that include saturation values as Gompertz logarithmic equations (Berger 1981, Fang et al. 2005). Though, their implementation requires previous knowledge of the process (starting values).

5.3 QuantReg Performance

This approach demonstrated to be convenient in detection of bush encroachment. One of the main advantages of QuantReg is its power to detect on-going ecological processes using limited variables (Cade and Noon 2003). In this study, two variables were used; NDVI and time both form the NDVI profiles. The aerial images are only required to corroborate or not perennial cover changes but are not necessary during the mathematical analysis.

QuantReg is the most accurate method to detect bush encroachment. It has a significant performance either to detect bush encroachment or to recognize No-Change pixels. An overall PCC of 0.77 is found in the 0.33 and 0.5 quantiles. The quantile 0.5 is the most appropriate to detect bush encroachment because it has the highest sensitivity whereas 0.33 quantile is the most accurate recognizing No-Change pixels with the highest specificity (Table 5). In this study, the power of QuantReg relies on its capacity to narrow the dataset to more informative subsets of the data. This provides a correct interpretation of NDVI increase caused by evergreen plants spread and not caused by other variables such as climatic variables.

In short, QuantReg demonstrates to be a consistent assessment of bush encroachment within the lowest quantiles which reveal increases of min.NDVI generated by perennial cover increase. It does the analysis based on the quantiles established by the researcher e.g. 0.25, 0.66 and it is independent of Orthophotos data.

5.4 Methods Comparison

All methods were validated using the same data set. However, the criteria used to define significant change varied among methods because each approach is based on different statistical techniques (Table 5). Nevertheless, pursuing to have an unbiased comparison it was decided to work with the default settings and the standard thresholds. CoverCAM ran with 1.0 (SD) threshold (de Bie et al. 2011, Ali et al. 2013). The same threshold was used in Cover-Fraction analysis. On the contrary, QuantReg requires a significance level which was fixed at 0.05. The sensitivity analysis and settings tuning were not within the scope of this research. Therefore, the analysis of the results is fixed to the performance of the methods under the default settings. The survey of new settings is a topic for further studies.

It is observed than min.NDVI interannual variability is stronger (Figure 16). This variation explains the low performance of CoverCAM because it includes the interannual variation of the reference period to perform the land cover change assessment in the monitoring period. Consequently, the changes caused by the spread of perennial vegetation are not large enough to be identified by CoverCAM. Moreover, the monitoring period of 5 years is likely to be not sufficient for brush encroachment assessment as it is a slow process. In the same way, Cover-Fraction shows a low performance. Cover-Fraction is not able to handle the NDVI interannual variability caused by other variables and leads to incorrect prediction of bush encroachment. It focuses on the min.NDVI values from the same years than the Orthophotos. This choice is made because of data availability and does not include any environmental reasoning. On the other hand, QuantReg excludes external variability e.g. climate, by separately analyzing the quantiles and thus is a strong method to detect bush encroachment in Cadiz.

This research shows a robust methodology that requires moderate resolution, free global MODIS 250m data, and has a significant detection of bush encroachment. Usually, studies of encroachment stand on areas that have information supporting bush encroachment occurrence and are performed at local scale. Mainly, these studies use high spatial resolution or hyperspectral imagery to measure reduction of evergreen vegetation gaps and species identification respectively (McGlynn and Okin 2006, Oldeland et al. 2010). But they are not applicable for large survey areas. By contrast, the QuantReg approach has the power to pinpoint areas with bush encroachment and has the potential to be applied at regional scale without knowledge whether the process is occurring or not. Further studies should aim at the development of an algorithm to assess bush encroachment detection in large areas using min.NDVI and QuantReg techniques.

Until now, it has not been applied any method to survey large areas to detect bush encroachment. Its accurate detection has become more relevant because it has been recognized as one of the major causes of habitat loss in biodiversity hotspots like the Mediterranean ecosystems (Plieninger 2006). Moreover, it is related to land degradation and land abandonment (Kunstler et al. 2007, Oldeland et al. 2010). Overall, detection of encroachment will bring out information for studies of biodiversity and land cover change caused by rural areas emigration and low agricultural productivity and profit.

Chapter 6. Conclusions, Limitations and Recommendations

6.1 Conclusion

- **The min.NDVI approach is a convenient method to detect bush encroachment** in Mediterranean ecosystems using the QuantReg method.
- **CoverCAM** using min.NDVI **has a bad performance** due to Interannual variability of min.NDVI negatively influences the detection of bush encroachment by. Tuning of the settings is required to increase the detection power of the method.
- **Cover-Fraction** of min. NDVI **approach is not adequate** for bush encroachment detection. Its dependency to Orthophotos determines its poor performance. Moreover, it is affected by environmental variables that are not part of this study and demand future investigation.
- **QuantReg** of min.NDVI **has a good potential** in surveying large areas to pinpoint bush encroachment at the pixel level. The increase of min.NDVI is consistent in the 0.33 and 0.5 quantiles for pixels with perennial vegetation.

6.2 Recommendations and Limitations

QuantReg should be used to survey other areas and improve its accuracy. Until now, its application is limited to Mediterranean ecosystems with evergreen perennial vegetation and annual vegetation that dried out or die in summer. For the other methods, further sensitivity analysis of the settings and thresholds (p-values, range of tolerance, weights) are recommended. Exploration of different weights or SD to assigned the tolerance range of CoverCAM and Cover-Fraction. They will provide a complete overview of the methods performance and improve their accuracy. It is strongly recommended to continue investigating QuantReg. Its good performance and its high detection of bush encroachment have demonstrated that is a robust technique which could be improved with further investigations. Also, exploration of other fractions of the NDVI profiles, could bring out new outcomes and basis for the analysis automation.

Literature

AEMET. 2012. Una primavera seca y cálida. Agencia Estatal de Metereología. Ministerio de Agricultura, Alimentación y Medio Ambiente. http://www.aemet.es/en/-s:pdf/noticias/2012/06/climaticoprimav2012.

Ali, A., C. A. J. M. de Bie, A. K. Skidmore, R. G. Scarrott, A. Hamad, V. Venus, and P. Lymberakis. 2013. Mapping land cover gradients through analysis of hyper-temporal NDVI imagery. International Journal of Applied Earth Observation and Geoinformation **23**:301-312.

Archer, S., D. S. Schimel, and E. A. Holland. 1995. Mechanisms of shrubland expansion: land use, climate or CO_2? Climatic Change **29**:91-99.

Beltran-Abaunza, J. M. 2009. Method development to prepare from hyper-temporla images semote sensing (RD)-base change maps. Master Thesis GEM program. ITC. Faculty of Geo-Information Science and Earth Observation.

University of Twente. 52p, Enschede - The Netherlands.

Berger, R. D. 1981. Comparison of the Gompertz and logistic equations to describe plant disease progress. Ecology and Epidemiology **71**:716-719.

Breusch, T. S. and A. R. Pagan. 1979. A Simple Test for Heteroscedasticity and Random Coefficient Variation. Econometrica **47**:1287-1294.

Busetto, L., M. Meroni, and R. Colombo. 2008. Combining medium and coarse spatial resolution satellite data to improve the estimation of sub-pixel NDVI time series. Remote Sensing of Environment **112**:118-131.

Büttner, G., B. Kosztra, G. Maucha, and R. Pataki. 2012. Implementation and achievments of CLC2006. European Environment Agency.

Cade, B. S. and B. R. Noon. 2003. A gentle introduction to quantile regression for ecologists. Frontiers in Ecology and the Environment **1**:412-420.

Candau, P., M. Carrasco, A. M. Pérez Tello, G. M. F.J., and J. Morales. 2002. Aerobiología en Andalucía: estación de cadíz (2000-2001). Rea **7**:43-48.

Cohen, W. B. and S. N. Goward. 2004. Landsat's Role in Ecological Applications of Remote Sensing. BioScience **54**:535-545.

Connell, J. H. and r. O. Slatyer. 1977. Mechanisms of sucession in natural communities and their role in community stability and organization. The American Naturalist **111**:26.

Consejería de Agricultura y Pesca. 2003. Anuario de Estadísticas Agrarias y Pesqueras de Andalucia. Junata de Andalucia. Viceconsejería Servicio de Publicación y Divulgación. Sevilla.

Consejeria de Medio Ambiente. 2010. Medio Ambiente en Andalucia. Informe 2010. Junta de Andalucia.

De Aranzabal, I., M. F. Schmitz, P. Aguilera, and F. D. Pineda. 2008. Modelling of landscape changes derived from the dynamics of socio-ecological systems: A case of study in a semiarid Mediterranean landscape. Ecological Indicators **8**:672-685.

de Bie, C. A. J. M., M. R. Khan, V. U. Smakhtin, V. Venus, M. J. C. Weir, and E. M. A. Smaling. 2011. Analysis of multi-temporal SPOT NDVI images for small-scale land-use mapping. International Journal of Remote Sensing **32**:6673-6693.

De Bie, C. A. J. M., M. R. Khan, A. G. Toxopeus, V. Venus, and A. K. Skidmore. 2008. Hypertemporal image analysis for crop mapping and change detection. The

International Archives of the Photogrammetry, Remote Sensing and Spatial Information Sciences. Vol. XXXVII. Part B7. Beijing 2008.

Decout, S., S. Manel, C. Miaud, and S. Luque. 2012. Integrative approach for landscape-based graph connectivity analysis: a case study with the common frog (<i>Rana temporaria) in human-dominated landscapes. Landscape Ecology **27**:267-279.

Díaz, M., F. J. Pulido, and T. Marañón. 2003. Diversidad biológica y sostenibilidad ecológica y económica de los sistemas adehesados. Ecosistemas **3**.

Diputacion de Cadiz. 2012. Diputación de Cadiz, La Provincia. Available on: http://www.dipucadiz.es/opencms/opencms/dipucadiz/provincia/ [Consulted on 23/08/2012].

Durbin, J. and G. S. Watson. 1971. Testing for serial correlation in least squares regression.III. Biometrika **58**:1-19.

EEA. 2010. Corine Land Cover 2006 raster data. European Environmental Agency, http://www.eea.europa.eu/data-and-maps/data/corine-land-cover-2006-raster Accessed August 2012.

Fang, J., S. Piao, L. Zhou, J. He, F. Wei, R. B. Myneni, C. J. Tucker, and K. Tan. 2005. Precipitation patterns alter growth of temperate vegetation. Geophysical Research Letters **32**:n/a-n/a.

Fischer, J. and D. B. Lindenmayer. 2007. Landscape modification and habitat fragmentation: a synthesis. Global Ecology and Biogeography **16**:265-280.

Folke, C., S. Carpenter, B. Walker, M. Scheffer, T. Elmqvist, L. Gunderson, and C. S. Holling. 2004. Regime Shifts, Resilience, and Biodiversity in Ecosystem Management. Annual Review of Ecology, Evolution, and Systematics **35**:557-581.

Geerken, R., B. Zaitchik, and J. P. Evans. 2005. Classifying rangeland vegetation type and coverage from NDVI time series using Fourier Filtered Cycle Similarity. International Journal of Remote Sensing **26**:5535-5554.

Geerken, R. A. 2009. An algorithm to classify and monitor seasonal variations in vegetation phenologies and their inter-annual change. ISPRS Journal of Photogrammetry and Remote Sensing **64**:422-431.

Hermance, J. F., R. W. Jacob, B. A. Bradley, and J. F. Mustard. 2007. Extracting Phenological Signals From Multiyear AVHRR NDVI Time Series: Framework for Applying High-Order Annual Splines With Roughness Damping. Geoscience and Remote Sensing, IEEE Transactions on **45**:3264-3276.

Hickler, T., L. Eklundh, J. W. Seaquist, B. Smith, J. Ardö, L. Olsson, M. T. Sykes, and M. Sjöström. 2005. Precipitation controls Sahel greening trend. Geophysical Research Letters **32**:L21415.

Hmimina, G., E. Dufrêne, J. Y. Pontailler, N. Delpierre, M. Aubinet, B. Caquet, A. de Grandcourt, B. Burban, C. Flechard, A. Granier, P. Gross, B. Heinesch, B. Longdoz, C. Moureaux, J. M. Ourcival, S. Rambal, L. Saint André, and K. Soudani. 2013. Evaluation of the potential of MODIS satellite data to predict vegetation phenology in different biomes: An investigation using ground-based NDVI measurements. Remote Sensing of Environment **132**:145-158.

Huete, A., C. Justice, and H. Liu. 1994. Development of vegetation and soil indices for MODIS-EOS. Remote Sensing of Environment **49**:224-234.

INE. 2012. Instituto Nacional de Estadítica. [website: http://www.ine.es/].

Jordán López, A., L. Martínez-Zavala, F. A. González Peñalosa, and N. Bellifante Crocci. 2008. Cambios de uso del suelo en la costa de la provincia de Cádiz durante la segunta mitad del siglo XX (1956-2003). Pages 1-18. Centro de Estudios Andaluces. Consejeria de Presidencia. Junta de Andalucia

Kawabata, A., K. Ichii, and Y. Yamaguchi. 2001. Global monitoring of interannual changes in vegetation activities using NDVI and its relationships to temperature and precipitation. International Journal of Remote Sensing **22**:1377-1382.

Kerr, J. T. and M. Ostrovsky. 2003. From space to species: ecological applications for remote sensing. Trends in Ecology & Evolution **18**:299-305.

Khan, M. R., C. A. J. M. de Bie, H. van Keulen, E. M. A. Smaling, and R. Real. 2010. Disaggregating and mapping crop statistics using hypertemporal remote sensing. International Journal of Applied Earth Observation and Geoinformation **12**:36-46.

Koenker, R. 2006. Quantile regression in R: A vignette. The Comprehensive R Archive Network. CRAN R project, http://cran.r-project.org/web/packages/quantreg/vignettes/rq.pdf.

Koenker, R. and G. Bassett. 1978. Regression quantiles. Econometrica: journal of the Econometric Society:33-50.

Kunstler, G., J. Chad uf, E. K. Klein, T. Curt, M. Bouchaud, and J. Lepart. 2007. Tree colonization of sub-Mediterranean grasslands: effects of dispersal limitation and shrub facilitation. Canadian Journal of Forest Research **37**:103-115.

Lasanta, T., J. Arnáez, M. Oserín, and L. M. Ortigosa. 2001. Marginal Lands and Erosion in Terraced Fields in the Mediterranean Mountains. Mountain Research and Development **21**:69-76.

Lassau, S. A., G. Cassis, P. K. J. Flemons, L. Wilkie, and D. F. Hochuli. 2005. Using high-resolution multi-spectral imagery to estimate habitat complexity in open-canopy forests: can we predict ant community patterns? Ecography **28**:495-504.

Lillesand, T. M., R. W. Kiefer, and J. W. Chipman. 2008. Remote sensing and image interpretation. Sixth edition edition. Wiley & Sons, New York.

Lunetta, R. S., J. F. Knight, J. Ediriwickrema, J. G. Lyon, and L. D. Worthy. 2006. Land-cover change detection using multi-temporal MODIS NDVI data. Remote Sensing of Environment **105**:142-154.

Marañón, T., R. Ajbilou, F. Ojeda, and J. Arroyo. 1999. Biodiversity of woody species in oak woodlands of southern Spain and northern Morocco. Forest Ecology and Management **115**:147-156.

McGlynn, I. O. and G. S. Okin. 2006. Characterization of shrub distribution using high spatial resolution remote sensing: Ecosystem implications for a former Chihuahuan Desert grassland. Remote Sensing of Environment **101**:554-566.

McIntyre, S. and R. Hobbs. 1999. A Framework for Conceptualizing Human Effects on Landscapes and Its Relevance to Management and Research Models. Conservation Biology **13**:1282-1292.

Moreno-Rueda, G. and M. Pizarro. 2007. Snake species richness and shrulands correlate with the short-toed eagle (*Circaetus gallicus*) in south-eastern Spain. Annales Zoologici Fennici **44**:314-320.

Myers, N., R. A. Mittermeier, C. G. Mittermeier, G. A. B. da Fonseca, and J. Kent. 2000. Biodiversity hotspots for conservation priorities. Nature **403**:853-858.

Naemi, M. 2012. Impact of user-settings on land cover change probability estimation (use of a prototype land cover change mapping method). Master thesis GEM program. ITC . Faculty of Geo-Information Science and Earth Observation.

University of Twente. p50, Enschede - The Netherlands.

Nguyen, T. T. H., C. A. J. M. De Bie, A. Ali, E. M. A. Smaling, and T. H. Chu. 2011. Mapping the irrigated rice cropping patterns of the Mekong delta, Vietnam, through hyper-temporal SPOT NDVI image analysis. International Journal of Remote Sensing **33**:415-434.

Oldeland, J., W. Dorigo, D. Wesuls, and N. Jürgens. 2010. Mapping Bush Encroaching Species by Seasonal Differences in Hyperspectral Imagery. Remote Sensing **2**:1416-1438.

Perez-Tris, J. and T. Santos. 2004. El estudio de la migración de aves en España: trayectoría histórica y perspectivas de futuro. Ardeola **51**:71-89.

Pickett, S. T. A., S. L. Collins, and J. J. Armesto. 1987. Models, mechanisms and pathways of succession. The Botanical Review **53**:335-371.

Plieninger, T. 2006. Habitat loss, Fragmentation, and Alteration – Quantifying the Impactof Land-use Changes on a Spanish Dehesa Landscape by Use of Aerial Photography and GIS. Landscape Ecology **21**:91-105.

Plieninger, T. and C. Wilbrand. 2001. Land use, biodiversity conservation, and rural development in the dehesas of Cuatro Lugares, Spain. Agroforestry Systems **51**:23-34.

Quinn, G. P. and M. Keough. 2005. Experimental Design and Data Analysis for Biologist. First edition. Fourth Printing. edition. Cambridge University Press, U. K. Cambridge.

Rewilding Europe. 2011. Western Iberia Project. Website: http://www.rewildingeurope.com/ Accessed on 08-22-2012.

Royston, P. 1995. Remark AS R94: A Remark on Algorithm AS 181: The W-test for Normality. Journal of the Royal Statistical Society. Series C (Applied Statistics) **44**:547-551.

Sanchez-Garcia, J. M., M. Navarro-Domingez, I. Marquez-Rodrigez, and M. A. Alavarez-Sotomayor. 2004. Arboles y arboladas singulares de Cadiz. Escandón impresores, Sevilla.

Sankaran, M., Niall P. Hanan, Robert J. Scholes, Jayashree Ratnam, David J. Augustine, Brian S. Cade, and J. G. e. al. 2005. Determinants of woody cover in African savannas. Nature **438**:846-849.

Scheffer, M. S. J. A. F. C. B. 2001. Catastrophic shifts in ecosystems. Nature **413**:591.

Sluiter, R. 2005. Mediterranean land cover change: Modelling and monitoring natural vegetation using GIS and remote sensing. Dotoral thesis. Utrecht University.

Sluiter, R. and S. de Jong. 2007. Spatial patterns of Mediterranean land abandonment and related land cover transitions. Landscape Ecology **22**:559-576.

Smith, B., P. Samuelsson, A. Wramneby, and M. Rummukainen. 2011. A model of the coupled dynamics of climate, vegetation and terrestrial ecosystem biogeochemistry for regional applications. Tellus A **63**:87-106.

Soudani, K., G. Hmimina, N. Delpierre, J. Y. Pontailler, M. Aubinet, D. Bonal, B. Caquet, A. de Grandcourt, B. Burban, C. Flechard, D. Guyon, A. Granier, P. Gross, B. Heinesh, B. Longdoz, D. Loustau, C. Moureaux, J. M. Ourcival, S. Rambal, L. Saint André, and E. Dufrêne. 2012. Ground-based Network of NDVI measurements for tracking temporal dynamics of canopy structure and vegetation phenology in different biomes. Remote Sensing of Environment **123**:234-245.

Srivastava, A. K. 2011. A novel approach of land cover change mapping using hyper temporal images. Master thesis GEM program. Master Thesis. ITC Faculty of Geo-Information Science and Earth Observation University of Twente. p66, Enschede.

Stellmes, M., T. Udelhoven, A. Röder, R. Sonnenschein, and J. Hill. 2010. Dryland observation at local and regional scale — Comparison of Landsat TM/ETM+ and NOAA AVHRR time series. Remote Sensing of Environment **114**:2111-2125.

Taiz, L. and E. Zeiger. 2010. Photosynthesis: The Light Reactions. Page 782 Plant Physiology. Sinauer Associates, Inc.

Terradas, J. 1991. Mediterranean woody plant growth-forms, biomass and production in the eastern part of the Iberian peninsula. Oecologia aquatica **10**:337-349.

Trexler, J., C. McCulloch, and J. Travis. 1988. How can the functional reponse best be determined? Oecologia **76**:206-214.

U. S. Geological Survey. 2011. Vegetation Indices 16-Day L3 Global 250m. https://lpdaac.usgs.gov/products/modis_products_table/mod13q1.

U. S. Geological Survey. 2012. Remote Sensing Phenology. NDVI from AVHRR. http://phenology.cr.usgs.gov/ndvi_avhrr.php.

Verbesselt, J., R. Hyndman, G. Newnham, and D. Culvenor. 2010. Detecting trend and seasonal changes in satellite image time series. Remote Sensing of Environment **114**:106-115.

Verburg, P. H., C. J. E. Schulp, N. Witte, and A. Veldkamp. 2006. Downscaling of land use change scenarios to assess the dynamics of European landscapes. Agriculture, Ecosystems & Environment **114**:39-56.

Vogiatzakis, I. N., A. M. Mannion, and G. H. Griffiths. 2006. Mediterranean ecosystems: problems and tools for conservation. Progress in Physical Geography **30**:175-200.

Weier, J. and D. Herrin. 2011. Measuring vegetation (NDVI & EVI). NASA Earth Observatory, http://earthobservatory.nasa.gov/Features/MeasuringVegetation/measuring_vegetation_1.php.

Zhan, X., R. A. Sohlberg, J. R. G. Townshend, C. DiMiceli, M. L. Carroll, J. C. Eastman, M. C. Hansen, and R. S. DeFries. 2002. Detection of land cover changes using MODIS 250 m data. Remote Sensing of Environment **83**:336-350.

Appendixes

7.1 Appendix I.

PIXELS WITH VEGETATION COVER LOSS
DETECTED BY COVERCAM

ID: 38264

2004 2006 2010

ID: 38264

2004 2006 2010

EXAMPLES OF CHANGE PIXELS

ID: 49152

2003 2005 2011

ID: 49153

2003 2005 2011

ID: 48888

2003 2005 2011

ID: 49715

2003 2005 2011

EXAMPLES OF NO-CHANGE PIXELS

ID: 43180

2001 2006 2010

ID: 49063

2001 2006 2010

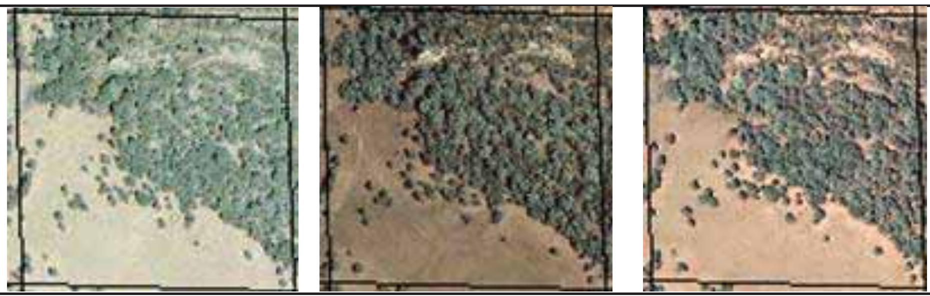

ID: 66671

2003 2005 2011

ID: 46894

2003 2005 2011

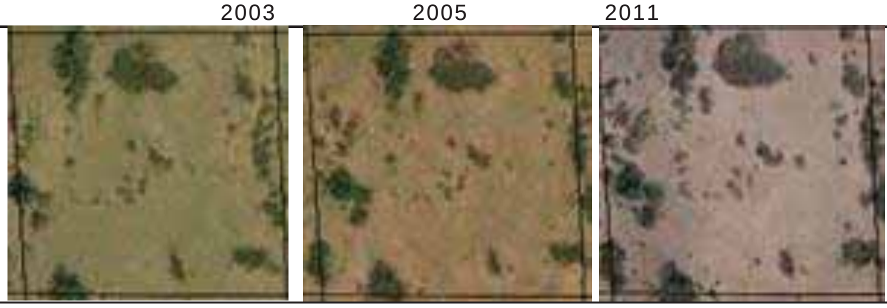

7.2 Appendix II.

CALIBRATION DATASET RESULTS OF QUANTREG

Table 7. QuantReg parameters and statistics of Change pixels. Calibration Dataset. β_0= intercept and β_1= slope. Degrees of freedom=34

px ID	Tao	β_0	β_1	t-value	p-value
1	0.25	140.78	0.04	0.89	0.38
1	0.33	147.52	0.03	0.64	0.53
1	0.5	153.92	0.04	1.05	0.30
1	0.66	166.42	-0.01	-0.43	0.67
1	0.75	167.47	-0.01	-0.24	0.81
2	0.25	143.34	0.09	2.12	0.04
2	0.33	146.81	0.07	1.75	0.09
2	0.5	155.05	0.07	1.82	0.08
2	0.66	158.10	0.06	2.75	0.01
2	0.75	156.65	0.12	4.03	0.00
3	0.25	129.69	0.04	1.16	0.25
3	0.33	133.00	0.08	2.03	0.05
3	0.5	138.44	0.07	2.06	0.05
3	0.66	143.38	0.06	1.57	0.13
3	0.75	148.67	0.04	1.10	0.28
4	0.25	141.65	0.07	2.27	0.03
4	0.33	146.17	0.05	1.43	0.16
4	0.5	150.96	0.07	2.05	0.05
4	0.66	154.24	0.09	2.83	0.01
4	0.75	155.39	0.10	3.84	0.00
5	0.25	128.48	0.09	4.85	0.00
5	0.33	129.35	0.09	4.47	0.00
5	0.5	131.75	0.08	2.76	0.01
5	0.66	137.28	0.09	2.67	0.01
5	0.75	139.34	0.09	2.24	0.03
6	0.25	136.47	0.07	3.89	0.00
6	0.33	137.61	0.07	2.73	0.01
6	0.5	140.48	0.07	2.87	0.01
6	0.66	140.65	0.12	3.54	0.00
6	0.75	141.94	0.12	3.70	0.00
7	0.25	100.46	0.11	3.78	0.00
7	0.33	102.46	0.11	4.64	0.00
7	0.5	105.22	0.11	4.10	0.00
7	0.66	112.36	0.09	2.81	0.01
7	0.75	114.92	0.08	2.03	0.05
8	0.25	98.73	0.05	2.02	0.05
8	0.33	99.52	0.07	3.05	0.00
8	0.5	102.50	0.07	3.19	0.00
8	0.66	109.73	0.04	1.36	0.18
8	0.75	109.12	0.06	1.49	0.15
9	0.25	117.11	0.11	4.52	0.00
9	0.33	119.62	0.10	4.25	0.00
9	0.5	119.93	0.12	6.37	0.00
9	0.66	126.18	0.10	5.23	0.00
9	0.75	128.21	0.10	4.86	0.00

px ID	Tao	β_0	β_1	t-value	p-value
10	0.25	116.66	0.10	5.27	0.00
10	0.33	116.35	0.11	6.39	0.00
10	0.5	119.96	0.10	7.66	0.00
10	0.66	123.39	0.09	5.88	0.00
10	0.75	123.11	0.10	5.77	0.00
11	0.25	105.73	0.06	2.75	0.01
11	0.33	106.54	0.07	4.09	0.00
11	0.5	113.51	0.04	1.97	0.06
11	0.66	116.75	0.04	1.37	0.18
11	0.66	116.75	0.04	1.37	0.18
11	0.75	117.78	0.04	0.96	0.34
12	0.25	127.89	0.02	0.65	0.52
12	0.33	127.80	0.04	1.37	0.18
12	0.5	128.33	0.06	2.77	0.01
12	0.66	133.17	0.04	2.16	0.04
12	0.75	134.06	0.04	1.60	0.12
13	0.25	142.49	0.05	4.59	0.00
13	0.33	142.75	0.06	4.06	0.00
13	0.5	145.20	0.06	2.21	0.03
13	0.66	146.52	0.08	2.53	0.02
13	0.75	153.59	0.06	1.90	0.07
14	0.25	144.42	0.05	1.50	0.14
14	0.33	143.31	0.09	2.64	0.01
14	0.5	147.22	0.13	4.63	0.00
14	0.66	149.22	0.13	4.21	0.00
14	0.75	150.09	0.13	5.70	0.00
15	0.25	158.48	0.05	2.02	0.05
15	0.33	157.87	0.07	3.73	0.00
15	0.5	157.58	0.09	4.97	0.00
15	0.66	161.50	0.07	5.20	0.00
15	0.75	161.42	0.08	3.69	0.00
16	0.25	88.80	0.04	3.39	0.00
16	0.33	89.55	0.05	2.88	0.01
16	0.5	93.68	0.03	1.71	0.10
16	0.66	99.90	0.02	0.89	0.38
16	0.75	99.83	0.03	1.43	0.16
17	0.25	107.90	0.04	1.59	0.12
17	0.33	108.00	0.06	2.60	0.01
17	0.5	109.64	0.06	2.53	0.02
17	0.66	113.74	0.05	1.92	0.06
17	0.75	126.00	0.00	0.00	1.00

Table 8. QuantReg parameters and statistics of No-Change pixels. Calibration Dataset. β_0= intercept and β_1= slope. Degrees of freedom=34

px (ID)	Tao	β_0	β_1	t-value	p-value		px (ID)	Tao	β_0	β_1	t-value	p-value
1	0.25	132.89	0.02	0.57	0.57		10	0.25	128.76	0.05	1.08	0.29
1	0.33	134.61	0.03	0.61	0.55		10	0.33	129.26	0.05	1.37	0.18
1	0.5	139.18	0.04	0.84	0.41		10	0.5	132.63	0.05	2.11	0.04
1	0.66	144.86	0.08	1.91	0.06		10	0.66	138.13	0.03	1.30	0.20
1	0.75	146.75	0.08	2.26	0.03		10	0.75	137.65	0.05	1.63	0.11
2	0.25	128.84	0.03	0.74	0.47		11	0.25	139.84	0.03	1.46	0.15
2	0.33	129.26	0.05	1.37	0.18		11	0.33	139.65	0.07	3.26	0.00
2	0.5	132.63	0.05	1.84	0.07		11	0.5	140.88	0.07	3.03	0.00
2	0.66	138.13	0.03	1.30	0.20		11	0.66	143.40	0.07	3.20	0.00
2	0.75	137.65	0.05	1.63	0.11		11	0.75	146.31	0.07	2.53	0.02
3	0.25	155.98	0.00	0.08	0.94		12	0.25	139.96	0.04	1.73	0.09
3	0.33	166.47	-0.02	-0.36	0.72		12	0.33	141.52	0.03	1.19	0.24
3	0.5	168.00	0.00	0.00	1.00		12	0.5	141.68	0.06	2.43	0.02
3	0.66	177.35	-0.04	-1.36	0.18		12	0.66	141.76	0.10	4.05	0.00
3	0.75	183.07	-0.06	-2.75	0.01		12	0.75	143.23	0.10	4.10	0.00
4	0.25	144.95	0.01	0.20	0.85		13	0.25	175.92	0.01	0.31	0.76
4	0.33	157.64	-0.01	-0.30	0.76		13	0.33	177.83	0.01	0.16	0.87
4	0.5	158.87	0.00	0.13	0.90		13	0.5	178.72	0.04	1.08	0.29
4	0.66	161.00	0.00	0.00	1.00		13	0.66	186.16	0.02	0.64	0.53
4	0.75	161.00	0.00	0.00	1.00		13	0.75	186.91	0.02	0.91	0.37
5	0.25	109.77	0.04	1.60	0.12		14	0.25	168.87	0.02	0.88	0.38
5	0.33	113.87	0.03	0.97	0.34		14	0.33	169.97	0.02	0.62	0.54
5	0.5	120.79	0.01	0.29	0.77		14	0.5	170.04	0.06	1.72	0.09
5	0.66	119.74	0.04	1.61	0.12		14	0.66	170.39	0.09	3.48	0.00
5	0.75	121.98	0.04	1.33	0.19		14	0.75	178.56	0.06	2.09	0.04
6	0.25	112.55	0.03	1.65	0.11		15	0.25	127.04	-0.01	-0.24	0.81
6	0.33	115.83	0.03	1.54	0.13		15	0.33	129.76	0.01	0.33	0.74
6	0.5	117.99	0.03	1.40	0.17		15	0.5	130.74	0.04	1.48	0.15
6	0.66	120.74	0.04	1.80	0.08		15	0.66	133.83	0.03	1.28	0.21
6	0.75	120.51	0.07	2.31	0.03		15	0.75	133.69	0.06	2.02	0.05
7	0.25	116.90	0.04	1.75	0.09		16	0.25	139.95	0.01	0.31	0.76
7	0.33	118.87	0.04	1.81	0.08		16	0.33	139.89	0.02	0.70	0.49
7	0.5	122.63	0.06	2.92	0.01		16	0.5	140.67	0.04	1.52	0.14
7	0.66	124.58	0.07	3.97	0.00		16	0.66	143.51	0.07	2.89	0.01
7	0.75	125.03	0.07	4.81	0.00		16	0.75	146.22	0.06	2.59	0.01
8	0.25	116.75	0.04	2.20	0.03		17	0.25	127.10	0.03	0.81	0.42
8	0.33	116.79	0.04	1.78	0.08			0.33				
8	0.5	123.50	0.01	0.46	0.65			0.5				
8	0.66	122.28	0.06	2.74	0.01			0.66				
8	0.75	122.69	0.06	4.05	0.00			0.75				
9	0.25	132.89	0.02	0.57	0.57							
9	0.33	134.61	0.03	0.61	0.55							
9	0.5	139.18	0.04	0.84	0.41							
9	0.66	144.86	0.08	1.91	0.06							
9	0.75	146.75	0.08	2.26	0.03							

CALIBRATION PLOTS

Change pixels

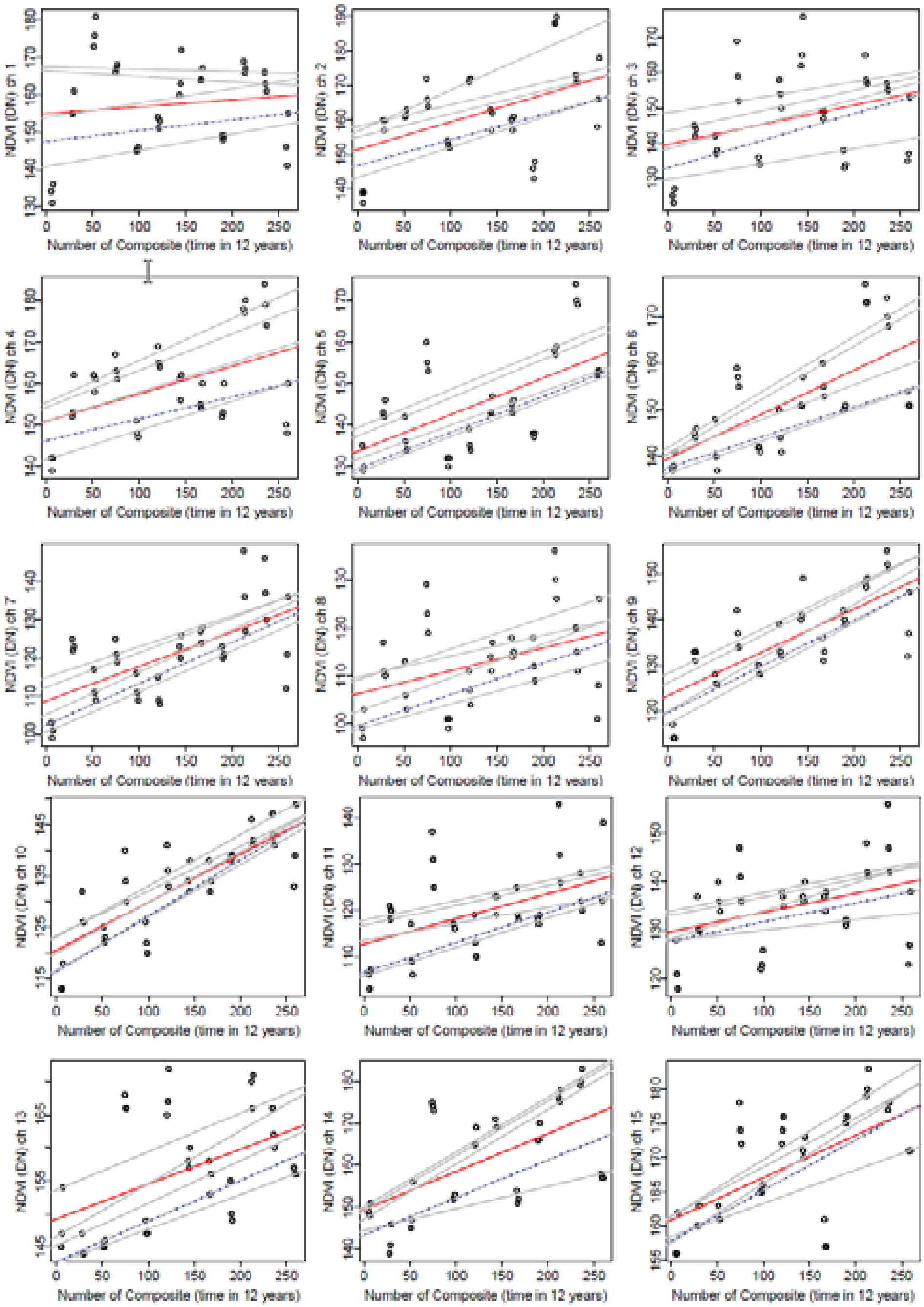

a.

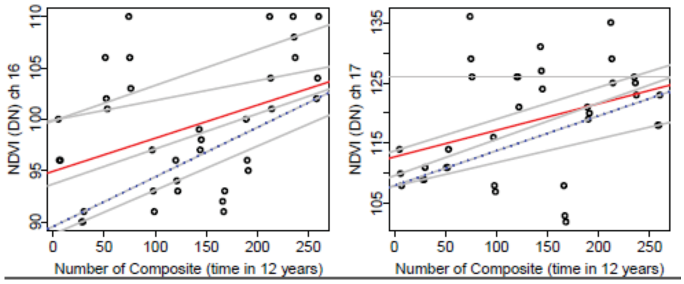

Figure 26. QuantReg plots of Change pixels. Calibration dataset. n=17. Red solid line is the standard linear regression. Blue dotted line is the 0.33 QuantReg and the Gray lines are the other quantiles

No-Change pixels

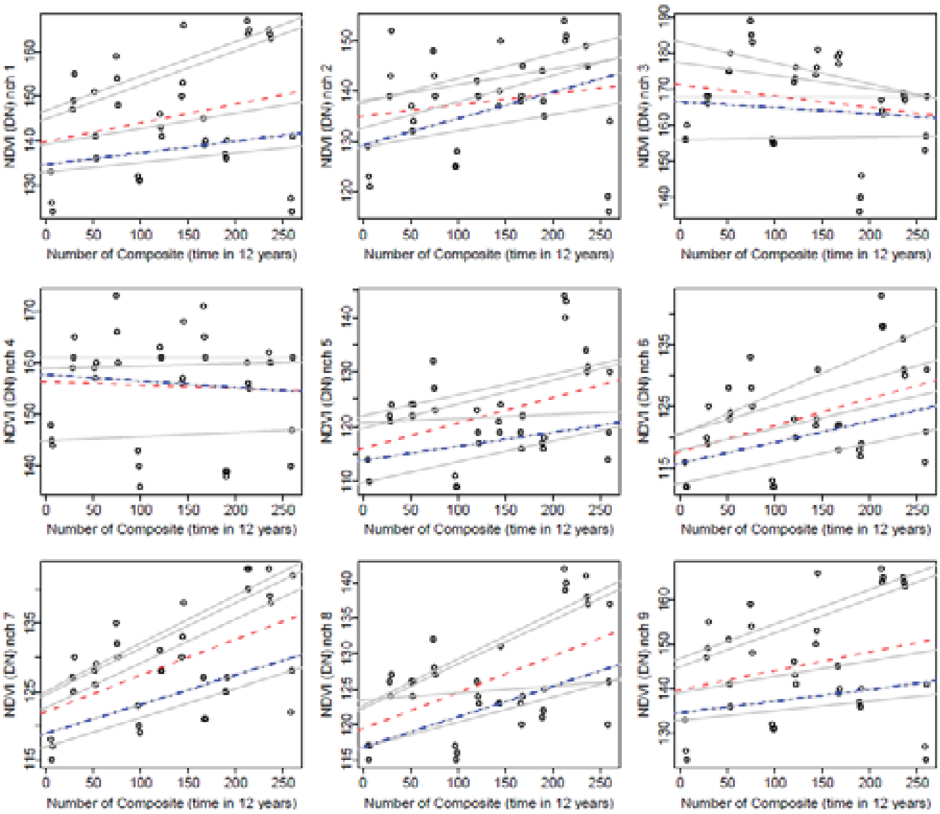

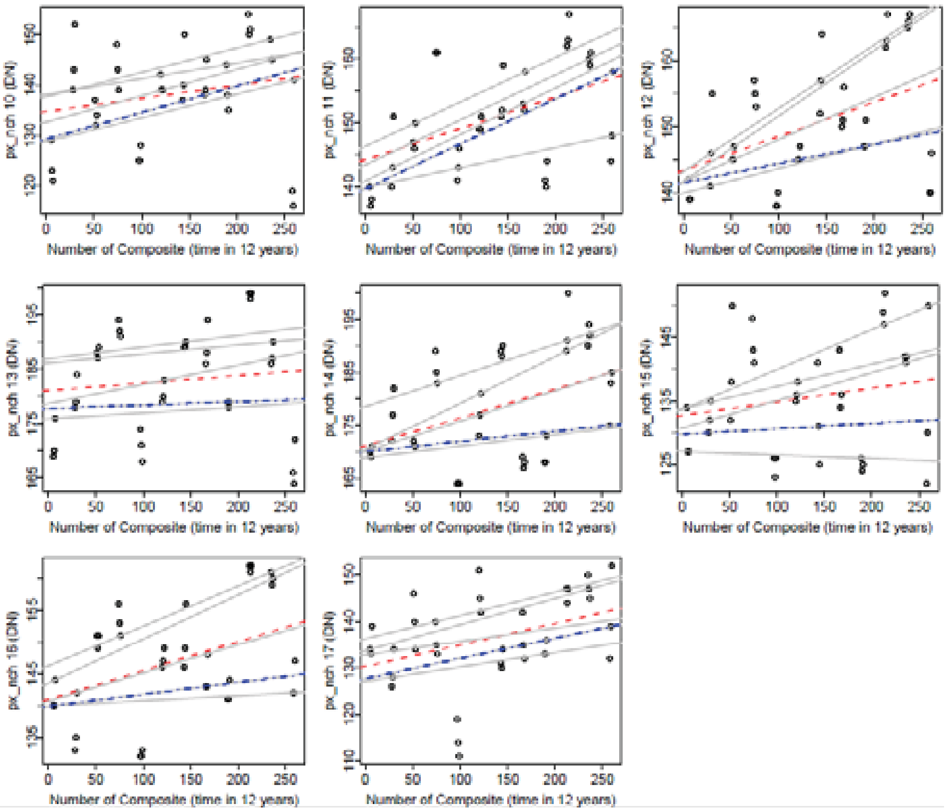

Figure 27. QuantReg plots of No-Change pixels n=17. Calibration dataset. Red pointed line is the standard linear regression. Blue dotted lines is the 0.33 QuantReg and the Gray lines are the other quantiles.

VALIDATION DATASET RESULTS

Table 9. QuantReg parameters and statistics of Change pixels. Validation dataset β_0=intercept β_1 =slope. Degrees of freedom=34

px (ID)	Tao	β_0	β_1	t-value	p-value
1	0.25	107.67	0.05	1.579	0.124
1	0.33	108.51	0.07	2.845	0.007
1	0.50	112.68	0.06	2.906	0.006
1	0.66	113.61	0.08	3.437	0.002
1	0.75	114.63	0.08	3.046	0.004
2	0.25	106.62	0.08	4.079	0.000
2	0.33	107.39	0.09	4.194	0.000
2	0.50	107.52	0.11	5.666	0.000
2	0.66	109.04	0.11	4.929	0.000
2	0.75	113.14	0.09	4.221	0.000
3	0.25	104.22	0.10	3.942	0.000
3	0.33	105.38	0.10	4.369	0.000
3	0.50	109.14	0.12	4.979	0.000
3	0.66	111.39	0.12	4.399	0.000
3	0.75	111.30	0.14	4.916	0.000
4	0.25	103.09	0.10	3.636	0.001
4	0.33	109.40	0.10	3.619	0.001
4	0.50	111.95	0.11	4.116	0.000
4	0.66	112.42	0.12	5.792	0.000
4	0.75	112.35	0.13	4.854	0.000
5	0.25	98.50	0.07	3.727	0.001
5	0.33	101.70	0.06	2.922	0.006
5	0.50	104.25	0.06	3.084	0.004
5	0.66	105.61	0.08	3.775	0.001
5	0.75	108.36	0.07	3.277	0.002
6	0.25	141.75	0.05	2.364	0.024
6	0.33	141.73	0.05	3.085	0.004
6	0.50	142.48	0.09	4.110	0.000
6	0.66	146.39	0.09	3.664	0.001
6	0.75	146.33	0.10	3.990	0.000
7	0.25	143.74	0.04	1.290	0.206
7	0.33	143.61	0.06	2.037	0.050
7	0.50	144.48	0.09	3.895	0.000
7	0.66	146.92	0.08	3.300	0.002
7	0.75	148.49	0.07	3.368	0.002
8	0.25	140.74	0.04	2.771	0.009
8	0.33	141.34	0.05	2.320	0.026
8	0.50	140.43	0.10	4.063	0.000
8	0.66	143.57	0.09	3.342	0.002
8	0.75	144.28	0.10	5.030	0.000
9	0.25	128.74	0.04	1.977	0.056
9	0.33	129.66	0.04	2.135	0.040
9	0.50	131.66	0.05	2.953	0.006
9	0.66	135.78	0.04	1.780	0.084
9	0.75	140.42	0.02	0.936	0.356
10	0.25	134.76	0.05	1.895	0.067
10	0.33	134.93	0.06	2.256	0.031
10	0.50	136.95	0.07	3.604	0.001
10	0.66	139.67	0.06	4.645	0.000
10	0.75	143.26	0.05	4.345	0.000
11	0.25	131.73	0.05	1.706	0.097
11	0.33	133.03	0.07	2.226	0.033
11	0.50	136.65	0.07	3.139	0.003
11	0.66	142.75	0.06	3.138	0.004
11	0.75	142.77	0.06	3.415	0.002
12	0.25	124.25	0.03	2.770	0.009
12	0.33	126.28	0.03	1.546	0.131
12	0.50	127.03	0.04	1.814	0.078
12	0.66	128.36	0.05	1.920	0.063
12	0.75	128.60	0.08	2.663	0.012
13	0.25	142.77	0.02	0.586	0.562
13	0.33	143.75	0.02	0.585	0.562
13	0.50	144.69	0.04	2.451	0.020
13	0.66	148.92	0.04	1.860	0.071
13	0.75	151.01	0.03	1.539	0.133
14	0.25	148.72	0.05	1.617	0.115
14	0.33	149.79	0.04	1.551	0.130
14	0.50	154.46	0.03	1.164	0.253
14	0.66	162.00	0.00	0.000	1.000
14	0.75	161.91	0.03	1.019	0.316
15	0.25	140.99	0.04	1.374	0.178
15	0.33	139.65	0.06	2.466	0.019
15	0.50	141.72	0.06	3.026	0.005
15	0.66	143.69	0.06	3.485	0.001
15	0.75	144.11	0.07	3.615	0.001
16	0.25	143.31	0.05	1.861	0.071
16	0.33	143.99	0.06	1.792	0.082
16	0.50	148.54	0.05	2.057	0.047
16	0.66	157.93	0.01	0.396	0.695
16	0.75	158.39	0.02	0.730	0.470
17	0.25	161.00	0.00	0.000	1.000
17	0.33	162.83	-0.01	-0.261	0.796
17	0.50	162.94	0.01	0.567	0.575
17	0.66	164.20	0.04	1.401	0.170
17	0.75	165.47	0.05	1.652	0.108

Table 10. Validation parameters and statistics of No-Change pixels for Linear QuantReg. β_0= intercept and β_1= slope. Degrees of freedom=34

px (ID)	Tao	β_0	β_1	t-value	p-value
1	0.25	156.25	0.00	-0.32	0.75
1	0.33	157.02	0.00	-0.19	0.85
1	0.5	159.30	0.02	0.98	0.34
1	0.66	163.67	0.01	0.44	0.66
1	0.75	163.02	0.03	1.63	0.11
2	0.25	145.93	0.01	0.47	0.64
2	0.33	145.87	0.03	0.90	0.37
2	0.5	147.46	0.05	2.19	0.04
2	0.66	151.75	0.04	1.27	0.21
2	0.75	152.45	0.05	1.91	0.06
3	0.25	145.75	0.04	1.13	0.27
3	0.33	145.69	0.05	1.56	0.13
3	0.5	150.75	0.04	1.48	0.15
3	0.66	151.58	0.06	2.39	0.02
3	0.75	151.39	0.09	3.33	0.00
4	0.25	128.11	-0.02	-1.00	0.33
4	0.33	128.03	-0.01	-0.23	0.82
4	0.5	128.90	0.02	0.94	0.35
4	0.66	131.83	0.02	0.80	0.43
4	0.75	132.01	0.03	1.26	0.21
5	0.25	121.17	-0.01	-0.16	0.87
5	0.33	120.39	0.02	0.62	0.54
5	0.5	134.11	-0.02	-0.68	0.50
5	0.66	135.67	-0.01	-0.65	0.52
5	0.75	138.07	-0.01	-0.68	0.50
6	0.25	108.61	0.01	0.56	0.58
6	0.33	117.12	-0.02	-0.79	0.44
6	0.5	120.55	-0.01	-0.43	0.67
6	0.66	122.00	0.00	0.00	1.00
6	0.75	123.00	0.00	0.00	1.00
7	0.25	134.15	-0.02	-1.06	0.30
7	0.33	134.43	-0.01	-0.53	0.60
7	0.5	134.76	0.05	1.80	0.08
7	0.66	137.74	0.04	1.18	0.25
7	0.75	142.29	0.02	1.29	0.21
8	0.25	140.22	-0.04	-3.20	0.00
8	0.33	140.30	-0.04	-1.82	0.08
8	0.5	141.95	0.01	0.29	0.77
8	0.66	145.00	0.00	0.00	1.00
8	0.75	152.56	-0.03	-1.34	0.19
9	0.25	125.51	-0.03	-0.95	0.35
9	0.33	125.98	-0.02	-0.85	0.40
9	0.5	125.21	0.03	1.59	0.12
9	0.66	126.83	0.03	1.41	0.17
9	0.75	127.77	0.04	2.36	0.02
10	0.25	145.24	0.07	1.75	0.09
10	0.33	145.77	0.07	2.04	0.05
10	0.5	156.64	0.06	1.99	0.05
10	0.66	154.49	0.11	4.50	0.00
10	0.75	156.35	0.11	5.65	0.00
11	0.25	152.78	0.01	0.51	0.61
11	0.33	154.97	0.01	0.22	0.83
11	0.5	155.06	0.04	1.53	0.14
11	0.66	155.83	0.06	2.28	0.03
11	0.75	158.00	0.07	2.83	0.01
12	0.25	149.58	0.07	2.43	0.02
12	0.33	150.23	0.07	2.51	0.02
12	0.5	150.42	0.12	4.02	0.00
12	0.66	155.30	0.10	3.07	0.00
12	0.75	156.37	0.12	4.55	0.00
13	0.25	149.24	0.05	2.06	0.05
13	0.33	150.67	0.05	2.40	0.02
13	0.5	151.04	0.07	2.32	0.03
13	0.66	156.61	0.08	3.16	0.00
13	0.75	161.53	0.06	2.18	0.04
14	0.25	106.67	0.01	0.73	0.47
14	0.33	110.00	0.00	0.00	1.00
14	0.5	109.95	0.01	0.52	0.61
14	0.66	112.91	0.02	0.64	0.52
14	0.75	115.25	0.01	0.36	0.72
15	0.25	143.13	-0.03	-1.44	0.16
15	0.33	144.17	-0.03	-1.52	0.14
15	0.5	144.17	-0.01	-0.24	0.81
15	0.66	143.93	0.03	1.02	0.31
15	0.75	146.79	0.03	1.00	0.33
16	0.25	163.08	-0.02	-0.83	0.41
16	0.33	163.00	0.00	0.00	1.00
16	0.5	162.78	0.04	1.68	0.10
16	0.66	167.90	0.04	1.40	0.17
16	0.75	171.10	0.03	1.40	0.17
17	0.25	126.14	-0.03	-1.27	0.21
17	0.33	126.13	-0.02	-0.97	0.34
17	0.5	129.00	-0.02	-1.09	0.28
17	0.66	128.97	0.00	0.24	0.81
17	0.75	132.00	0.00	0.00	1.00
18	0.25	154.77	-0.01	-0.68	0.50
18	0.33	155.26	-0.01	-0.34	0.74
18	0.5	157.41	-0.01	-0.27	0.79
18	0.66	159.94	0.01	0.38	0.70
18	0.75	160.45	0.01	0.42	0.68
19	0.25	162.92	0.02	0.56	0.58
19	0.33	167.00	0.00	0.00	1.00
19	0.5	170.85	0.02	0.72	0.48
19	0.66	174.72	0.01	0.33	0.75
19	0.75	173.75	0.04	2.14	0.04
20	0.25	123.53	0.02	0.62	0.54
20	0.33	124.93	0.01	0.45	0.66
20	0.5	125.34	0.02	1.03	0.31
20	0.66	129.04	0.01	0.57	0.57
20	0.75	133.29	-0.01	-0.23	0.82
21	0.25	112.42	-0.01	-0.48	0.63
21	0.33	122.34	-0.06	-1.66	0.11
21	0.5	125.96	-0.06	-2.29	0.03
21	0.66	129.32	-0.06	-1.96	0.06
21	0.75	133.64	-0.07	-2.57	0.01
22	0.25	110.69	-0.02	-0.84	0.41
22	0.33	111.02	0.00	-0.16	0.88
22	0.5	116.05	-0.02	-0.54	0.59
22	0.66	117.57	-0.01	-0.39	0.70
22	0.75	120.28	-0.01	-0.19	0.85

px (ID)	Tao	β_0	β_1	t-value	p-value
23	0.25	128.00	0.00	0.00	1.00
23	0.33	126.57	0.01	0.55	0.59
23	0.5	128.81	0.03	1.22	0.23
23	0.66	134.02	0.04	1.02	0.32
23	0.75	134.28	0.04	1.05	0.30
24	0.25	132.10	-0.02	-0.90	0.38
24	0.33	132.37	-0.01	-0.71	0.48
24	0.5	133.00	0.00	0.00	1.00
24	0.66	133.87	0.03	0.81	0.42
24	0.75	137.37	0.01	0.45	0.66
25	0.25	111.67	0.01	0.34	0.74
25	0.33	111.33	0.02	0.76	0.45
25	0.5	123.02	0.00	-0.15	0.88
25	0.66	124.95	0.01	0.36	0.72
25	0.75	128.41	0.01	0.54	0.59
26	0.25	125.04	-0.01	-0.64	0.53
26	0.33	124.80	0.01	0.56	0.58
26	0.5	125.26	0.02	1.18	0.25
26	0.66	128.71	0.01	0.38	0.71
26	0.75	132.03	0.00	-0.30	0.76
27	0.25	123.60	0.06	4.16	0.00
27	0.33	123.51	0.07	5.71	0.00
27	0.5	125.07	0.07	5.43	0.00
27	0.66	126.81	0.06	5.56	0.00
27	0.75	127.80	0.07	5.51	0.00
28	0.25	110.24	0.03	2.95	0.01
28	0.33	111.81	0.03	3.48	0.00
28	0.5	111.97	0.04	3.23	0.00
28	0.66	111.78	0.04	5.14	0.00
28	0.75	113.08	0.04	4.33	0.00
29	0.25	118.12	0.03	4.75	0.00
29	0.33	119.53	0.03	2.77	0.01
29	0.5	119.84	0.03	3.49	0.00
29	0.66	121.79	0.03	2.73	0.01
29	0.75	122.42	0.03	2.50	0.02

px (ID)	Tao	β_0	β_1	t-value	p-value
30	0.25	151.71	0.06	2.46	0.02
30	0.33	151.68	0.06	4.42	0.00
30	0.5	155.31	0.06	3.00	0.01
30	0.66	157.12	0.06	2.78	0.01
30	0.75	156.97	0.10	3.36	0.00
31	0.25	148.00	0.00	0.00	1.00
31	0.33	148.91	0.01	0.40	0.69
31	0.5	148.63	0.05	1.46	0.15
31	0.66	158.43	0.01	0.30	0.76
31	0.75	159.13	0.02	0.56	0.58
32	0.25	166.03	0.00	-0.13	0.90
32	0.33	169.78	-0.01	-0.47	0.64
32	0.5	172.17	-0.01	-0.26	0.80
32	0.66	174.16	-0.01	-0.26	0.79
32	0.75	178.43	-0.02	-1.05	0.30
33	0.25	153.78	0.04	2.22	0.03
33	0.33	157.81	0.03	1.59	0.12
33	0.5	159.75	0.04	1.84	0.07
33	0.66	161.79	0.04	1.78	0.08
33	0.75	163.63	0.04	1.61	0.12
34	0.25	143.34	0.05	2.66	0.01
34	0.33	145.77	0.04	1.49	0.15
34	0.5	145.73	0.05	2.41	0.02
34	0.66	150.67	0.05	2.22	0.03
34	0.75	158.68	0.02	0.65	0.52
35	0.25	157.23	-0.04	-1.78	0.08
35	0.33	157.20	-0.03	-1.93	0.06
35	0.5	159.81	-0.04	-1.40	0.17
35	0.66	160.04	-0.01	-0.27	0.79
35	0.75	159.86	0.03	0.93	0.36

VALIDATION PLOTS

Change pixels

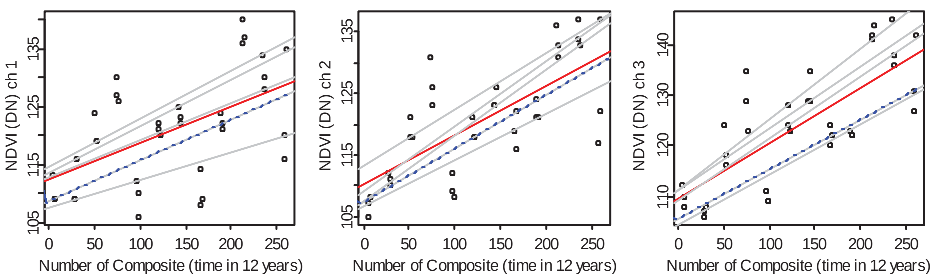

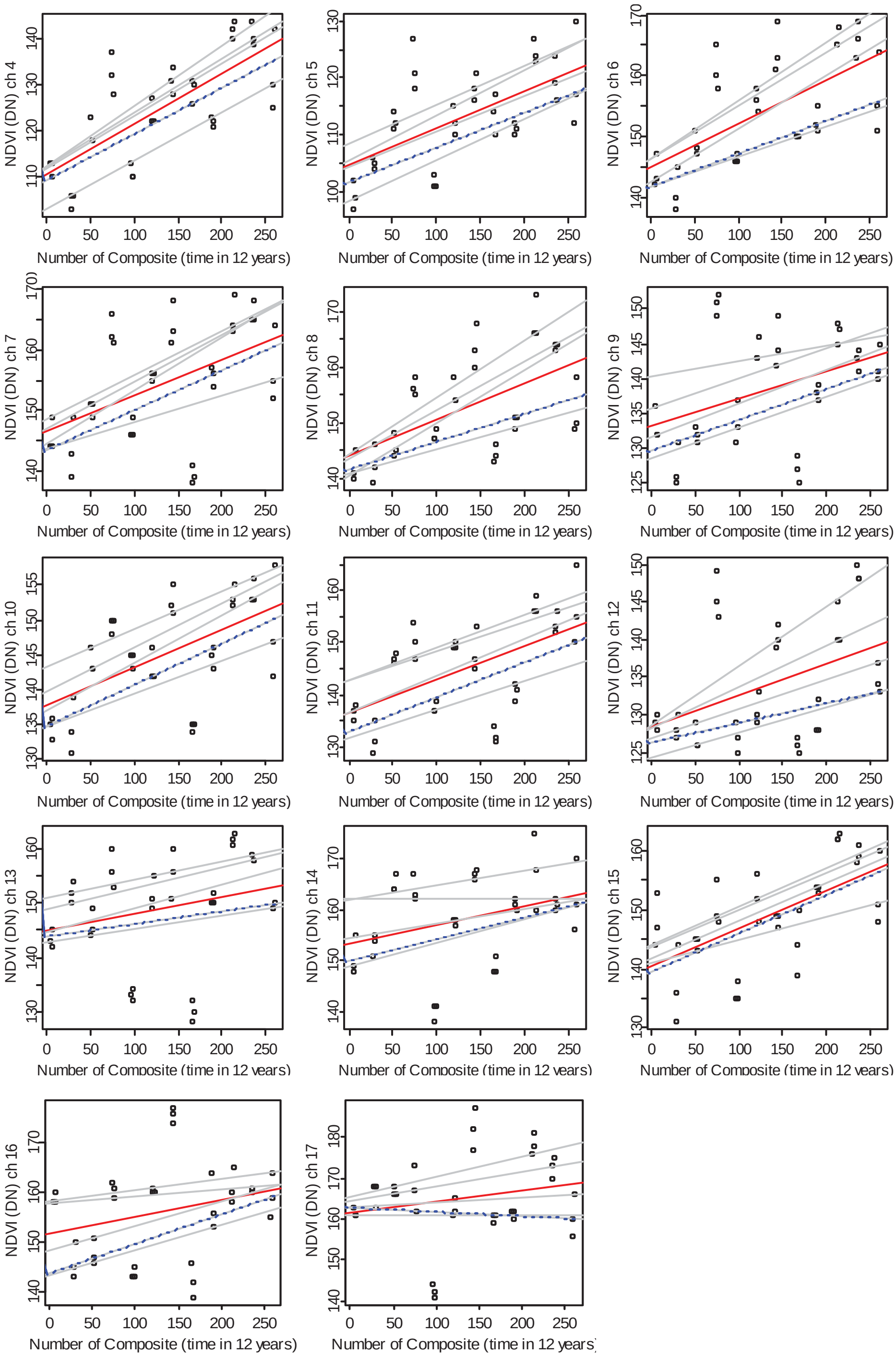

Figure 28. QuantReg plots of Change pixels n=17. Validation dataset. Red line standard linear regression. Blue dotted line: 0.33 quantile. Gray lines: other quantiles

No-Change pixels

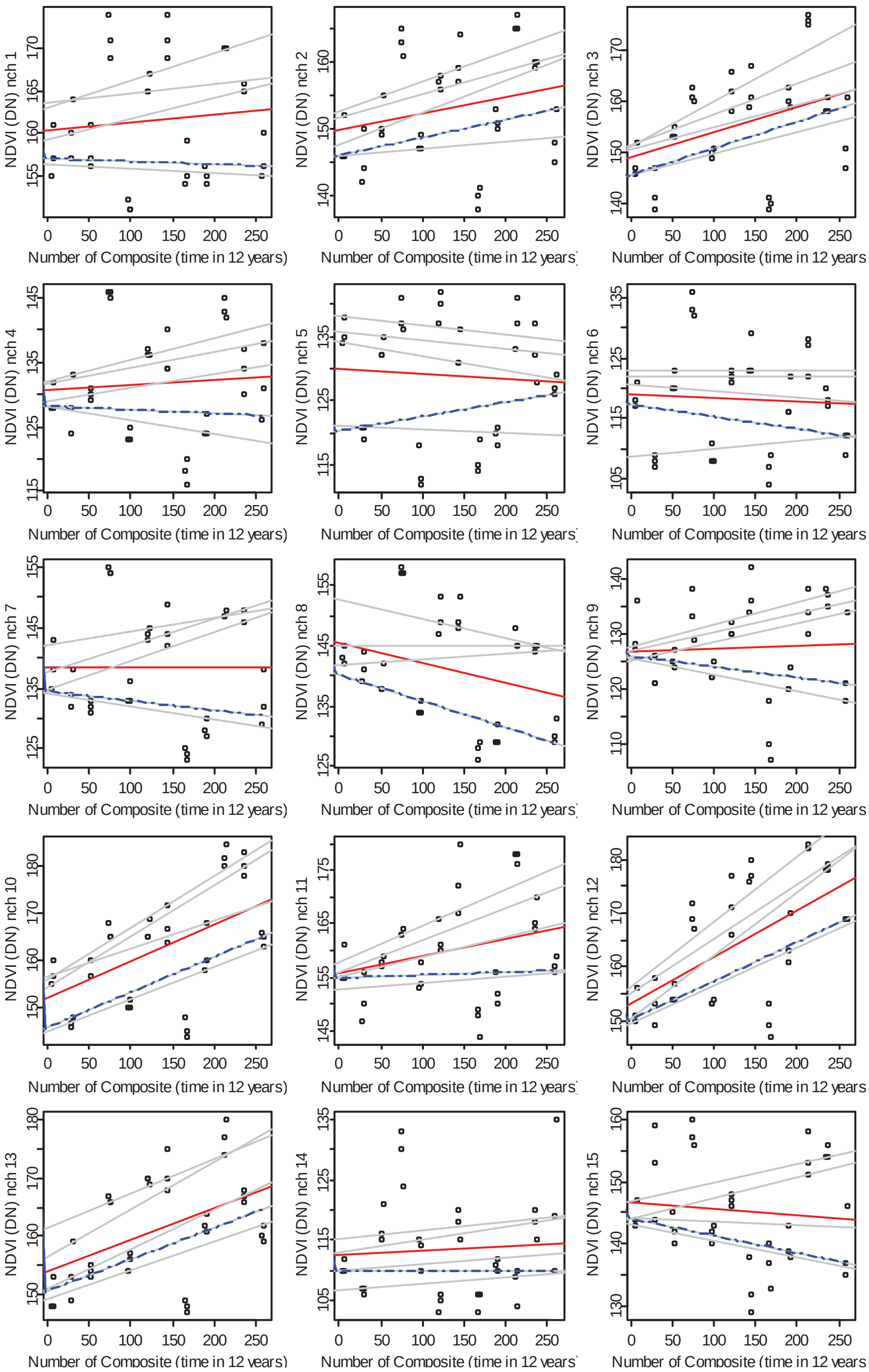

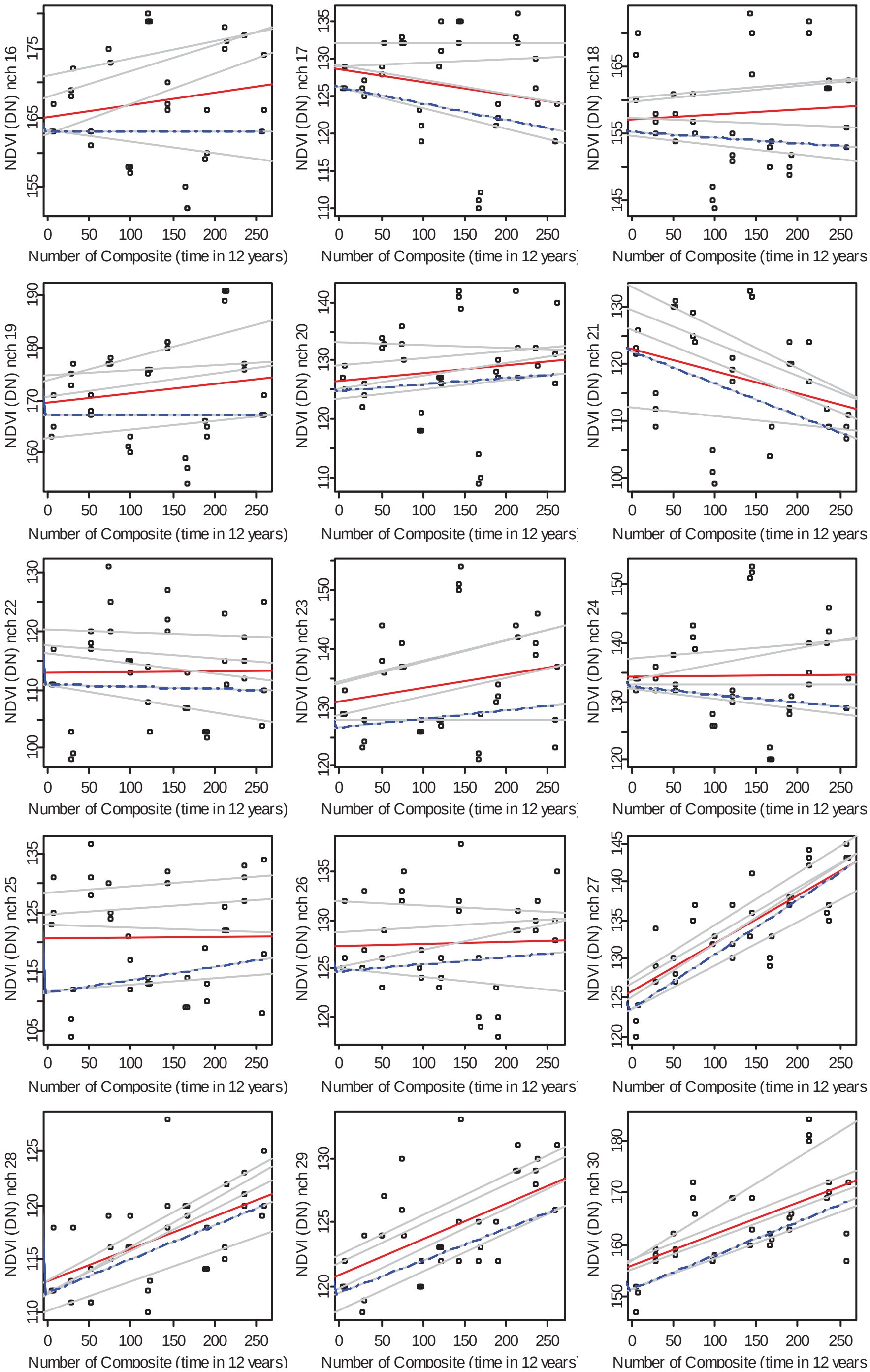
NDVI (DN) nch 16
NDVI (DN) nch 17
NDVI (DN) nch 18
NDVI (DN) nch 19
NDVI (DN) nch 20
NDVI (DN) nch 21
NDVI (DN) nch 22
NDVI (DN) nch 23
NDVI (DN) nch 24
NDVI (DN) nch 25
NDVI (DN) nch 26
NDVI (DN) nch 27
NDVI (DN) nch 28
NDVI (DN) nch 29
NDVI (DN) nch 30
Number of Composite (time in 12 years)

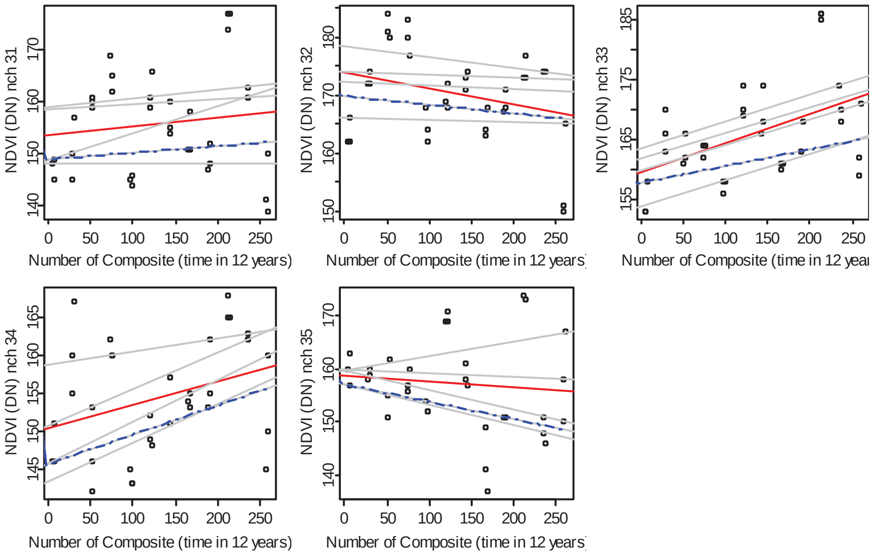

Figure 29. QuantReg plots of No-Change pixels n=17. Validation dataset. Red line is the standard linear regression. Blue dotted line is the 0.33 QuantReg and the Gray lines are the other quantiles.